IET Control Theory & Applications

Research Article

IET Journals
The Institution of Engineering and Technology

Two-stage unscented Kalman filter algorithm for fault estimation in spacecraft attitude control system

ISSN 1751-8644
Received on 8th December 2017
Revised 13th March 2018
Accepted on 3rd April 2018
E-First on 15th May 2018
doi: 10.1049/iet-cta.2017.1369
www.ietdl.org

Xueqin Chen[1], Rui Sun[1] ✉, Feng Wang[1], Daozhe Song[1], Wancheng Jiang[1]

[1]*Research Center of Satellite Technology, Harbin Institute of Technology, Harbin 150006, People's Republic of China*

✉ *E-mail: srada@163.com*

Abstract: The study of fault/bias estimation based on the two-stage Kalman filter and the unscented Kalman filter in the presence of unknown random biases is addressed. Two kinds of faults are taken into account: additive faults and multiplicative faults, which are modelled as actuator faults and sensor faults in the spacecraft attitude control system (ACS). In accordance with the characteristic of the fault model of ACS, where the system state and the faults are decoupled, a novel two-stage unscented Kalman filter (TSUKF) algorithm is developed to estimate the decoupled states and biases simultaneously. By employing the unscented transform, the TSUKF algorithm does not need any linearisation of non-linear system models or the augmentation of the state, contributing to a more precise estimation. Meanwhile the computational cost is reduced by exploiting the bias-separate principle. The simulation results demonstrate the proposed algorithm when a micro-spacecraft is tracking a stable/manoeuvring target.

1 Introduction

The concept of the separate-bias estimation algorithm, which is also called two-stage Kalman filter (TSKF), is basically to estimate the states and the unknown constant biases of a linear system separately, and to obtain the optimal estimation using the coupling relationship between them. Since Friedland first proposed the separate-bias estimation algorithm [1], many related research have been conducted to achieve the optimal solution of TSKF. Alouani *et al.* [2] presented an algebraic constraint on the correlation between the state process and bias noises considering a white Gaussian bias noise correlated with the system noise. Keller and Darouach [3] suggested an optimal solution of TSKF called OTSKF which can be used to estimate the optimal state and the optimal random bias, and further developed a two-stage optimal strategy for discrete-time stochastic linear systems subject to intermittent unknown inputs [4]. Based on OTSKF, Hsieh [5] proposed a robust TSKFRTSKF which was unaffected by the unknown inputs, and the estimation results were optimal and with high accuracy. Later, Khabbazi and Esfanjani [6] introduced the gain projection notion as a type of state constraint to RTSKF, further enhancing the accuracy. Based on the above improvements, nowadays the TSKF algorithm is widely used for fault estimation. Through defining the control effectiveness factors to represent the multiplicative faults, Hajiyev [7] extended the fault estimation to the estimation of control distribution matrix elements, so that the TSKF could be applied to actuator/surface fault diagnosis and fault-tolerant control of F-16. Wang and Qi [8] introduced two adaptive factors to the bias-free filter and bias filter, and presented a fault diagnosis strategy for flight control systems based on the closed-loop subspace model identification algorithm and the adaptive TSKF.

However, the above mentioned algorithms are not feasible for the fault estimation of non-linear system. To solve that problem, much dedication have been made to extended Kalman filter (EKF)-based linearisation approach. Qian *et al.* [9] proposed a robust EKF (REKF) to estimate the spacecraft attitude under the influence of multiplicative noises and unknown external disturbances. To deal with the uncertainty problem of non-linear estimation, Inoue *et al.* [10] designed another REKF suitable for online applications, by combining the robust regularisation and the penalty function together. Xiao *et al.* [11] presented a two-stage REKF for state estimation of non-linear uncertain system with unknown inputs and verified the good performance of the method in the powered descent phase of Mars EDL (entry, descent and landing). Xiao *et al.* [12] proposed an augmented robust three-stage EKF algorithm for Mars entry-phase autonomous navigation. However, due to the error produced by the interruption of higher dimensional terms in the Taylor series expansion, EKF is not suitable for high-dimensioned applications in many cases.

To improve the accuracy of non-linear filtering algorithm, the well-known unscented Kalman filter (UKF) [13] is chosen as there is no need for linearisation and the accuracy can reach as much as third-order to the Gaussian noise. Basically, to deal with the problem of fault diagnosis for the systems with non-linear state transition and observation models, the normal way is to formulate the original UKF in its augmented form, consisting of the coupled state and the bias. For instance, Rahimi *et al.* [14] used the adaptive UKF for state estimation [including angular velocity and reaction wheel (RW) parameters] for high-fidelity reaction wheel dynamics. Another way is to design a set of UKFs for different faults. Chatterjee *et al.* [15] used a bank of self-switched UKF to detect and to identify the faults in hybrid non-linear system. By using UKF instead of unknown input EKF for state estimation, the mode observer is avoided and lower latency and higher range coverage are achieved. Xiao *et al.* [16] proposed a robust three-stage UKF to deal with the situation that the statistical properties are partially known or unknown.

However, if the bias is decoupled from the state, just similar to the additive noise decoupled from the state, the problem can be simplified. For example, the non-augmented UKF was derived and employed to reduce the computational complexity in the special case where the process and the measurement noises were additive [17]; the marginalised iterated UKF was presented to simplify the iteration in the UKF with additive measurement noise, which reduced the computational burden [18]. Similarly, Xu *et al.* [19] proposed a two-stage UKF (TSUKF) to estimate the state and fault/bias. However, the linearisation steps still existed in the filtering process and detailed derivation was not given yet. Based on the widely used non-augmented UKF, in this study, the algorithm of TSUKF is improved to simultaneously estimate the decoupled state and the fault/bias. By introducing the separate-bias principle, the dimension of the states is reduced, leading to lower amount of computation. In addition, the unscented transform (UT) transformation is used in the TSUKF algorithm to achieve higher accuracy for non-linear system.

The contents of this paper are organised as follows. Section 2 proposes TSUKF with detailed derivation process; the ACS model with decoupled faults is described in Section 3 to examine three representative cases and analyse the numerical simulation results to evaluate the method. At last, the conclusions are drawn in Section 4.

2 TSUKF-based estimator

Consider a general form of the non-linear discrete-time stochastic system with a linear fault/bias

$$\begin{cases} \boldsymbol{x}_{k+1} = \boldsymbol{f}_k(\boldsymbol{x}_k) + \boldsymbol{F}_k^{\mathrm{a}}\boldsymbol{b}_k + \boldsymbol{w}_k^{\boldsymbol{x}} \\ \boldsymbol{b}_{k+1} = \boldsymbol{b}_k + \boldsymbol{w}_k^{\boldsymbol{b}} \\ \boldsymbol{y}_k = \boldsymbol{h}_k(\boldsymbol{x}_k) + \boldsymbol{F}_k^{\mathrm{s}}\boldsymbol{b}_k + \boldsymbol{v}_k \end{cases} \tag{1}$$

where $\boldsymbol{x}_k \in R^n$ is the state vector; $\boldsymbol{b}_k \in R^p$ is the fault/bias vector; $\boldsymbol{y}_k \in R^m$ is the measurement vector; $\boldsymbol{f}_k(\cdot)$ and $\boldsymbol{h}_k(\cdot)$ are non-linear functions; $\boldsymbol{F}_k^{\mathrm{a}} \in R^{n\times p}$ and $\boldsymbol{F}_k^{\mathrm{s}} \in R^{m\times p}$ are the fault distribution matrices. Without loss of generality, assume that the process noises, $\boldsymbol{w}_k^{\boldsymbol{x}}$ and $\boldsymbol{w}_k^{\boldsymbol{b}}$, and the measurement noise $\boldsymbol{v}_k$ are zero-mean Gaussian noise sequences with

$$E\left(\begin{bmatrix} \boldsymbol{w}_k^{\boldsymbol{x}} \\ \boldsymbol{w}_k^{\boldsymbol{b}} \\ \boldsymbol{v}_k \end{bmatrix}\begin{bmatrix} \boldsymbol{w}_j^{\boldsymbol{x}\mathrm{T}} & \boldsymbol{w}_j^{\boldsymbol{b}\mathrm{T}} & \boldsymbol{v}_j^{\mathrm{T}} \end{bmatrix}\right) = \begin{bmatrix} \boldsymbol{W}^{\boldsymbol{x}} & & \\ & \boldsymbol{W}^{\boldsymbol{b}} & \\ & & \boldsymbol{V} \end{bmatrix}\delta_{k,j}$$

where $\boldsymbol{W}^{\boldsymbol{x}} > 0$, $\boldsymbol{W}^{\boldsymbol{b}} > 0$, $\boldsymbol{V} > 0$, and $\delta_{k,j}$ is the Kronecker delta. The initial states $\boldsymbol{x}_0$ and $\boldsymbol{b}_0$ are assumed to be Gaussian random variables uncorrelated with the white noise processes given by

$$\begin{aligned} &\hat{\boldsymbol{x}}_0 = E(\boldsymbol{x}_0), \quad \boldsymbol{P}_0^{\boldsymbol{x}} = E\big(\boldsymbol{x}_0 - \hat{\boldsymbol{x}}_0\big)\big(\boldsymbol{x}_0 - \hat{\boldsymbol{x}}_0\big)^{\mathrm{T}} \\ &\hat{\boldsymbol{b}}_0 = E(\boldsymbol{b}_0), \quad \boldsymbol{P}_0^{\boldsymbol{b}} = E\Big(\boldsymbol{b}_0 - \hat{\boldsymbol{b}}_0\Big)\Big(\boldsymbol{b}_0 - \hat{\boldsymbol{b}}_0\Big)^{\mathrm{T}} \\ &\boldsymbol{P}_0^{\boldsymbol{x}\boldsymbol{b}} = E\big(\boldsymbol{x}_0 - \hat{\boldsymbol{x}}_0\big)\Big(\boldsymbol{b}_0 - \hat{\boldsymbol{b}}_0\Big)^{\mathrm{T}} \end{aligned}$$

A novel TSUKF is designed to estimate system information and actuator/sensor faults without linearisation of system models. The standard UKF using the augmented state is first applied, and then the filter is separated into a bias filter, a bias-free filter, their coupling equations and thereby a final compensated state filter.

Theorem 1: When the non-linear discrete-time stochastic system model with unknown bias is given by (1), a discrete-time TSUKF is given by the following coupled difference equations:

$$\begin{aligned} \hat{\boldsymbol{x}}_{k+1|k+1} &= \tilde{\boldsymbol{x}}_{k+1|k+1} + \boldsymbol{\beta}_{k+1|k+1}\hat{\boldsymbol{b}}_{k+1|k+1} \\ \boldsymbol{P}_{k+1|k+1}^{\boldsymbol{x}} &= \tilde{\boldsymbol{P}}_{k+1|k+1}^{\boldsymbol{x}} + \boldsymbol{\beta}_{k+1|k+1}\boldsymbol{P}_{k+1|k+1}^{\boldsymbol{b}}\boldsymbol{\beta}_{k+1|k+1}^{\mathrm{T}} \end{aligned} \tag{2}$$

The bias filter is

$$\begin{aligned} \hat{\boldsymbol{b}}_{k+1|k+1} &= \hat{\boldsymbol{b}}_{k+1|k} + \boldsymbol{K}_{k+1}^{\boldsymbol{b}}\big(\boldsymbol{y}_{k+1} - \hat{\boldsymbol{y}}_{k+1|k}\big) \\ \boldsymbol{P}_{k+1|k+1}^{\boldsymbol{b}} &= \boldsymbol{P}_{k+1|k}^{\boldsymbol{b}} - \boldsymbol{K}_{k+1}^{\boldsymbol{b}}\boldsymbol{P}_{k+1|k}^{\boldsymbol{y}\boldsymbol{y}}\boldsymbol{K}_{k+1}^{\boldsymbol{b}\mathrm{T}} \\ \boldsymbol{K}_{k+1}^{\boldsymbol{b}} &= \boldsymbol{P}_{k+1|k}^{\boldsymbol{b}\boldsymbol{y}}\big(\boldsymbol{P}_{k+1|k}^{\boldsymbol{y}\boldsymbol{y}}\big)^{-1} \\ \boldsymbol{P}_{k+1|k}^{\boldsymbol{y}\boldsymbol{y}} &= \tilde{\boldsymbol{P}}_{k+1|k}^{\boldsymbol{y}\boldsymbol{y}} + \boldsymbol{H}_{k+1|k}\boldsymbol{P}_{k+1|k}^{\boldsymbol{b}}\boldsymbol{H}_{k+1|k}^{\mathrm{T}} \\ \boldsymbol{P}_{k+1|k}^{\boldsymbol{b}\boldsymbol{y}} &= \boldsymbol{P}_{k+1|k}^{\boldsymbol{b}}\boldsymbol{H}_{k+1|k}^{\mathrm{T}} \\ \hat{\boldsymbol{y}}_{k+1|k} &= \boldsymbol{n}_{k+1} + \boldsymbol{F}_{k+1}^{\mathrm{s}}\hat{\boldsymbol{b}}_{k+1|k} \\ \boldsymbol{P}_{k+1|k}^{\boldsymbol{b}} &= \boldsymbol{P}_{k|k}^{\boldsymbol{b}} + \boldsymbol{W}_k^{\boldsymbol{b}} \\ \hat{\boldsymbol{b}}_{k+1|k} &= \hat{\boldsymbol{b}}_{k|k} \end{aligned} \tag{3}$$

the bias-free filter is

$$\begin{aligned} \tilde{\boldsymbol{x}}_{k+1|k+1} &= \tilde{\boldsymbol{x}}_{k+1|k} + \tilde{\boldsymbol{K}}_{k+1}^{\boldsymbol{x}}\big(\boldsymbol{y}_{k+1} - \tilde{\boldsymbol{y}}_{k+1|k}\big) \\ \tilde{\boldsymbol{P}}_{k+1|k+1}^{\boldsymbol{x}} &= \tilde{\boldsymbol{P}}_{k+1|k}^{\boldsymbol{x}} - \tilde{\boldsymbol{K}}_{k+1}^{\boldsymbol{x}}\tilde{\boldsymbol{P}}_{k+1|k}^{\boldsymbol{y}\boldsymbol{y}}\tilde{\boldsymbol{K}}_{k+1}^{\boldsymbol{x}\mathrm{T}} \\ \tilde{\boldsymbol{K}}_{k+1}^{\boldsymbol{x}} &= \tilde{\boldsymbol{P}}_{k+1|k}^{\boldsymbol{x}}\boldsymbol{N}_{k+1}^{\mathrm{T}}\big(\tilde{\boldsymbol{P}}_{k+1|k}^{\boldsymbol{y}\boldsymbol{y}}\big)^{-1} \\ \tilde{\boldsymbol{P}}_{k+1|k}^{\boldsymbol{y}\boldsymbol{y}} &= \sum_{i=0}^{2n}\omega_c^{\boldsymbol{x}(i)}\boldsymbol{\gamma}_{k+1}^{(i)}\boldsymbol{\gamma}_{k+1}^{(i)\ \mathrm{T}} \\ &\quad -\boldsymbol{N}_{k+1}\boldsymbol{\beta}_{k+1|k}\boldsymbol{P}_{k+1|k}^{\boldsymbol{b}}\boldsymbol{\beta}_{k+1|k}^{\mathrm{T}}\boldsymbol{N}_{k+1}^{\mathrm{T}} + \boldsymbol{V}_k \\ \boldsymbol{\gamma}_{k+1}^{(i)} &= \boldsymbol{h}_{k+1}\big(\boldsymbol{\chi}_{k+1|k}^{\boldsymbol{x}\ (i)}\big) - \boldsymbol{n}_{k+1} \\ \tilde{\boldsymbol{y}}_{k+1|k} &= \boldsymbol{n}_{k+1} - \boldsymbol{N}_{k+1}\boldsymbol{\beta}_{k+1|k}\hat{\boldsymbol{b}}_{k+1|k} \\ \boldsymbol{n}_{k+1} &= \sum_{i=0}^{2n}\omega_s^{\boldsymbol{x}(i)}\boldsymbol{h}_{k+1}\big(\boldsymbol{\chi}_{k+1|k}^{\boldsymbol{x}\ (i)}\big) \\ \tilde{\boldsymbol{P}}_{k+1|k}^{\boldsymbol{x}} &= \boldsymbol{P}_{k+1|k}^{\boldsymbol{x}} - \boldsymbol{\beta}_{k+1|k}\boldsymbol{P}_{k+1|k}^{\boldsymbol{b}}\boldsymbol{\beta}_{k+1|k}^{\mathrm{T}} \\ \tilde{\boldsymbol{x}}_{k+1|k} &= \hat{\boldsymbol{x}}_{k+1|k} - \boldsymbol{\beta}_{k+1|k}\hat{\boldsymbol{b}}_{k+1|k} \\ \boldsymbol{P}_{k+1|k}^{\boldsymbol{x}} &= \sum_{i=0}^{2n}\omega_c^{\boldsymbol{x}(i)}\Big[\boldsymbol{f}_k\big(\boldsymbol{\chi}_k^{\boldsymbol{x}(i)}\big) - \boldsymbol{m}_k\Big]\Big[\boldsymbol{f}_k\big(\boldsymbol{\chi}_k^{\boldsymbol{x}(i)}\big) - \boldsymbol{m}_k\Big]^{\mathrm{T}} \\ &\quad -\boldsymbol{M}_k\boldsymbol{\beta}_{k|k}\boldsymbol{P}_{k|k}^{\boldsymbol{b}}\boldsymbol{\beta}_{k|k}^{\mathrm{T}}\boldsymbol{M}_k^{\mathrm{T}} + \boldsymbol{R}_k\boldsymbol{P}_{k|k}^{\boldsymbol{b}}\boldsymbol{R}_k^{\mathrm{T}} + \boldsymbol{W}_k^{\boldsymbol{x}} \\ \hat{\boldsymbol{x}}_{k+1|k} &= \boldsymbol{m}_k + \boldsymbol{F}_k^{\mathrm{a}}\hat{\boldsymbol{b}}_{k|k} \\ \boldsymbol{m}_k &= \sum_{i=0}^{2n}\omega_s^{\boldsymbol{x}(i)}\boldsymbol{f}_k\big(\boldsymbol{\chi}_k^{\boldsymbol{x}(i)}\big) \end{aligned} \tag{4}$$

and the coupling equations are

$$\begin{aligned} \boldsymbol{\beta}_{k+1|k+1} &= \boldsymbol{\beta}_{k+1|k} - \tilde{\boldsymbol{K}}_{k+1}^{\boldsymbol{x}}\boldsymbol{H}_{k+1|k} \\ \boldsymbol{H}_{k+1|k} &= \boldsymbol{N}_{k+1}\boldsymbol{\beta}_{k+1|k} + \boldsymbol{F}_{k+1}^{\mathrm{s}} \\ \boldsymbol{\beta}_{k+1|k} &= \boldsymbol{R}_k\boldsymbol{P}_{k|k}^{\boldsymbol{b}}\big(\boldsymbol{P}_{k|k}^{\boldsymbol{b}} + \boldsymbol{W}_k^{\boldsymbol{b}}\big)^{-1} \\ \boldsymbol{R}_k &= \boldsymbol{M}_k\boldsymbol{\beta}_{k|k} + \boldsymbol{F}_k^{\mathrm{a}} \end{aligned} \tag{5}$$

where

$$\begin{aligned} \boldsymbol{M}_k &= \frac{1}{2\sqrt{3}\alpha} \\ &\quad \times \left\{\sum_{i=1}^{n}\Big[\boldsymbol{f}_k\big(\boldsymbol{\chi}_k^{\boldsymbol{x}(i)}\big) - \boldsymbol{f}_k\big(\boldsymbol{\chi}_k^{\boldsymbol{x}(i+n)}\big)\Big]\boldsymbol{e}_i^{\mathrm{T}}\right\}\big(\sqrt{\boldsymbol{P}_{k|k}^{\boldsymbol{x}}}\big)^{-1} \\ \boldsymbol{N}_{k+1} &= \frac{1}{2\sqrt{3}\alpha} \\ &\quad \times \left\{\sum_{i=1}^{n}\Big[\boldsymbol{h}_{k+1}\big(\boldsymbol{\chi}_{k+1|k}^{\boldsymbol{x}\ (i)}\big) - \boldsymbol{h}_{k+1}\big(\boldsymbol{\chi}_{k+1|k}^{\boldsymbol{x}\ (i+n)}\big)\Big]\boldsymbol{e}_i^{\mathrm{T}}\right\} \\ &\quad \times \big(\sqrt{\boldsymbol{P}_{k+1|k}^{\boldsymbol{x}}}\big)^{-1} \end{aligned} \tag{6}$$

where the sigma points are

$$\begin{aligned} \boldsymbol{\chi}_k^{\boldsymbol{x}(0)} &= \hat{\boldsymbol{x}}_{k|k} \\ \boldsymbol{\chi}_k^{\boldsymbol{x}(i)} &= \hat{\boldsymbol{x}}_{k|k} \pm \sqrt{(n+\lambda)\boldsymbol{P}_{k|k}^{\boldsymbol{x}}}\boldsymbol{e}_i \end{aligned} \tag{7}$$

and

$$\begin{aligned} \boldsymbol{\chi}_{k+1|k}^{\boldsymbol{x}\ (0)} &= \hat{\boldsymbol{x}}_{k+1|k} \\ \boldsymbol{\chi}_{k+1|k}^{\boldsymbol{x}\ (i)} &= \hat{\boldsymbol{x}}_{k+1|k} \pm \sqrt{(n+\lambda)\boldsymbol{P}_{k+1|k}^{\boldsymbol{x}}}\boldsymbol{e}_i \end{aligned} \tag{8}$$

where $i = 1, 2, \ldots, n$; $\sqrt{(n+\lambda)\boldsymbol{P}_{k|k}^{\boldsymbol{x}}}$ and $\sqrt{(n+\lambda)\boldsymbol{P}_{k+1|k}^{\boldsymbol{x}}}$ are the matrix square root of $(n+\lambda)\boldsymbol{P}_{k|k}^{\boldsymbol{x}}$ and $(n+\lambda)\boldsymbol{P}_{k+1|k}^{\boldsymbol{x}}$, respectively; the ith element of $\boldsymbol{e}_i$ is 1 while the others are 0; the corresponding weights are

$$\omega_s^{x(0)} = \frac{\lambda}{n+\lambda}, \quad \omega_c^{x(0)} = \frac{\lambda}{n+\lambda} + 1 - \alpha^2 + \beta$$
$$\omega_s^{x(i)} = \omega_c^{(i)} = \frac{1}{2(n+\lambda)}, \quad i = 1, 2, \ldots, 2n \tag{9}$$

where $\lambda = \alpha^2(n+\kappa) - n$, $\alpha \in [1 \times 10^{-4}, 1)$, $\kappa = 3 - n$, and $\beta = 2$.

Proof: To facilitate the derivations, define $\boldsymbol{X}_k = [(\boldsymbol{x}_k)^{\mathrm{T}}, (\boldsymbol{b}_k)^{\mathrm{T}}]^{\mathrm{T}}$, $\boldsymbol{w}_k = [(\boldsymbol{w}_k^{\boldsymbol{x}})^{\mathrm{T}}, (\boldsymbol{w}_k^{\boldsymbol{b}})^{\mathrm{T}}]^{\mathrm{T}}$, and the system model (1) can be rewritten as follows:

$$\begin{cases} \boldsymbol{X}_{k+1} = \boldsymbol{F}_k(\boldsymbol{X}_k) + \boldsymbol{w}_k \\ \qquad = \begin{bmatrix} \boldsymbol{f}_k(\boldsymbol{x}_k) + \boldsymbol{F}_k^{\mathrm{a}}\boldsymbol{b}_k \\ \boldsymbol{b}_k \end{bmatrix} + \begin{bmatrix} \boldsymbol{w}_k^{\boldsymbol{x}} \\ \boldsymbol{w}_k^{\boldsymbol{b}} \end{bmatrix} \\ \boldsymbol{y}_k = \boldsymbol{H}_k(\boldsymbol{X}_k) + \boldsymbol{v}_k \\ \qquad = \boldsymbol{h}_k\big(\begin{bmatrix} \boldsymbol{I}_n & \boldsymbol{0}_{n\times p} \end{bmatrix}\boldsymbol{X}_k\big) + \begin{bmatrix} \boldsymbol{0}_{m\times n} & \boldsymbol{F}_k^{\mathrm{s}} \end{bmatrix}\boldsymbol{X}_k + \boldsymbol{v}_k \end{cases} \tag{10}$$

where

$$\boldsymbol{W} = E\left(\begin{bmatrix} \boldsymbol{w}_k^{\boldsymbol{x}} \\ \boldsymbol{w}_k^{\boldsymbol{b}} \end{bmatrix}\begin{bmatrix} \boldsymbol{w}_j^{\boldsymbol{x}\mathrm{T}} & \boldsymbol{w}_k^{\boldsymbol{b}\mathrm{T}} \end{bmatrix}\right) = \begin{bmatrix} \boldsymbol{W}^{\boldsymbol{x}} & \\ & \boldsymbol{W}^{\boldsymbol{b}} \end{bmatrix}\delta_{k,j}$$

Define $L = n + p$, and the UKF algorithm is then used to estimate the system states of (10). The estimation steps are given as follows. First, calculate the $(2L+1)$ sigma points of the augmented state $\boldsymbol{X_k}$ by using the following equations:

$$\begin{aligned} &\chi_k^{(0)} = \hat{\boldsymbol{X}}_{k|k} \\ &\chi_k^{(i)} = \hat{\boldsymbol{X}}_{k|k} \pm (\sqrt{(L+\lambda)\boldsymbol{P}_{k|k}})_i, \quad i = 1, 2, \ldots, L \\ &\omega_s^{(0)} = \frac{\lambda}{L+\lambda}, \quad \omega_c^{(0)} = \frac{\lambda}{L+\lambda} + 1 - \alpha^2 + \beta \\ &\omega_s^{(i)} = \omega_c^{(i)} = \frac{1}{2(L+\lambda)}, \quad i = 1, 2, \ldots, 2L \end{aligned} \tag{11}$$

where $\lambda = \alpha^2(L+\kappa) - L$, $\alpha \in [1 \times 10^{-4}, 1)$, $\kappa = 3 - L$, $\beta = 2$, and $(\sqrt{(L+\lambda)\boldsymbol{P}_{k|k}})_i$ is the ith column of the matrix square root of $(L+\lambda)\boldsymbol{P}_{k|k}$.

Second, calculate the one-step prediction and the contrivance matrix as follows:

$$\boldsymbol{\chi}_{k+1|k}^{*(i)} = \boldsymbol{F}_k(\boldsymbol{\chi}_k^{(i)}), \quad i = 0, 1, 2, \ldots, 2L \tag{12}$$

$$\hat{\boldsymbol{X}}_{k+1|k} = \sum_{i=0}^{2L} \omega_s^{(i)} \boldsymbol{\chi}_{k+1|k}^{*(i)} \tag{13}$$

$$\boldsymbol{P}_{k+1|k} = \boldsymbol{W}_k + \sum_{i=0}^{2L} \omega_c^{(i)} \left(\boldsymbol{\chi}_{k+1|k}^{*(i)} - \hat{\boldsymbol{X}}_{k+1|k}\right)\left(\boldsymbol{\chi}_{k+1|k}^{*(i)} - \hat{\boldsymbol{X}}_{k+1|k}\right)^{\mathrm{T}} \tag{14}$$

The sigma points for $\hat{\boldsymbol{X}}_{k+1|k}$ can be then computed as follows:

$$\begin{aligned} &\boldsymbol{\chi}_{k+1|k}^{(0)} = \hat{\boldsymbol{X}}_{k+1|k} \\ &\boldsymbol{\chi}_{k+1|k}^{(i)} = \hat{\boldsymbol{X}}_{k+1|k} \pm (\sqrt{(L+\lambda)\boldsymbol{P}_{k+1|k}})_i, \quad i = 1, 2, \ldots, L \end{aligned} \tag{15}$$

With the obtained sigma points of $\boldsymbol{X}_{k+1|k}$, the one-step prediction of measurement, $\hat{\boldsymbol{y}}_{k+1|k}$, can be given by

$$\boldsymbol{y}_{k+1|k}^{(i)} = \boldsymbol{H}_k(\boldsymbol{\chi}_{k+1|k}^{(i)}), \quad i = 0, 1, \ldots, 2L \tag{16}$$

$$\hat{\boldsymbol{y}}_{k+1|k} = \sum_{i=0}^{2L} \omega_s^{(i)} \boldsymbol{y}_{k+1|k}^{(i)} \tag{17}$$

Finally, calculate the update of states and the contrivance matrix as follows:

$$\boldsymbol{P}_{k+1|k}^{\boldsymbol{yy}} = \boldsymbol{V}_k + \sum_{i=0}^{2L} \omega_c^{(i)} \left(\boldsymbol{y}_{k+1|k}^{(i)} - \hat{\boldsymbol{y}}_{k+1|k}\right)\left(\boldsymbol{y}_{k+1|k}^{(i)} - \hat{\boldsymbol{y}}_{k+1|k}\right)^{\mathrm{T}} \tag{18}$$

$$\boldsymbol{P}_{k+1|k}^{\boldsymbol{X}\boldsymbol{y}} = \sum_{i=0}^{2L} \omega_c^{(i)} \left(\boldsymbol{\chi}_{k+1|k}^{(i)} - \hat{\boldsymbol{X}}_{k+1|k}\right)\left(\boldsymbol{y}_{k+1|k}^{(i)} - \hat{\boldsymbol{y}}_{k+1|k}\right)^{\mathrm{T}} \tag{19}$$

$$\boldsymbol{K}_{k+1} = \boldsymbol{P}_{k+1}^{\boldsymbol{X}\boldsymbol{y}} \left(\boldsymbol{P}_{k+1}^{\boldsymbol{y}\boldsymbol{y}}\right)^{-1} \tag{20}$$

$$\hat{\boldsymbol{X}}_{k+1|k+1} = \hat{\boldsymbol{X}}_{k+1|k} + \boldsymbol{K}_{k+1}\left(\boldsymbol{y}_{k+1} - \hat{\boldsymbol{y}}_{k+1|k}\right) \tag{21}$$

$$\boldsymbol{P}_{k+1|k+1} = \boldsymbol{P}_{k+1|k} - \boldsymbol{K}_{k+1}\boldsymbol{P}_{k+1}^{\boldsymbol{y}\boldsymbol{y}}\boldsymbol{K}_{k+1}^{\mathrm{T}} \tag{22}$$

where

$$\boldsymbol{P}_{k|k} = \begin{bmatrix} \boldsymbol{P}_{k|k}^{\boldsymbol{x}} & \boldsymbol{P}_{k|k}^{\boldsymbol{x}\boldsymbol{b}} \\ \boldsymbol{P}_{k|k}^{\boldsymbol{b}\boldsymbol{x}} & \boldsymbol{P}_{k|k}^{\boldsymbol{b}} \end{bmatrix}$$

where $\boldsymbol{P}_{k|k}^{\boldsymbol{x}\boldsymbol{b}}$ and $\boldsymbol{P}_{k|k}^{\boldsymbol{b}\boldsymbol{x}}$ are non-diagnal matrices.

With (10)–(22), $\hat{\boldsymbol{X}}_{k+1}$ can be estimated by using the UKF algorithm, the next step is therefore to separate the original state and the bias from the estimation results. To achieve this, a transformation of the states is introduced, and the transform matrix is designed as

$$\boldsymbol{T} = \begin{bmatrix} \boldsymbol{I}_n & -\boldsymbol{\beta}_{k+1|k} \\ \boldsymbol{0}_{p\times n} & \boldsymbol{I}_p \end{bmatrix} \tag{23}$$

where

$$\boldsymbol{\beta}_{k+1|k} = \boldsymbol{P}_{k+1|k}^{\boldsymbol{x}\boldsymbol{b}} (\boldsymbol{P}_{k+1|k}^{\boldsymbol{b}})^{-1} \tag{24}$$

With this transformation, a new set of argument states and a diagonal matrix of $\boldsymbol{P}_{k+1|k}$ are given as follows:

$$\boldsymbol{T}\boldsymbol{X}_{k+1|k} = \boldsymbol{T}\begin{bmatrix} \hat{\boldsymbol{x}}_{k+1|k} \\ \hat{\boldsymbol{b}}_{k+1|k} \end{bmatrix} = \begin{bmatrix} \hat{\boldsymbol{x}}_{k+1|k} - \boldsymbol{\beta}_{k+1|k}\hat{\boldsymbol{b}}_{k|k} \\ \hat{\boldsymbol{b}}_{k|k} \end{bmatrix} \tag{25}$$

and

$$\boldsymbol{T}\boldsymbol{P}_{k+1|k}\boldsymbol{T}^{\mathrm{T}} = \begin{bmatrix} \boldsymbol{P}_{k+1|k}^{\boldsymbol{x}} - \boldsymbol{\beta}_{k+1|k}\boldsymbol{P}_{k+1|k}^{\boldsymbol{b}}\boldsymbol{\beta}_{k+1|k}^{\mathrm{T}} & \boldsymbol{0} \\ \boldsymbol{0} & \boldsymbol{P}_{k+1|k}^{\boldsymbol{b}} \end{bmatrix} \tag{26}$$

Define two new variables – the bias-free state and its covariance

$$\tilde{\boldsymbol{x}}_{k+1|k} = \hat{\boldsymbol{x}}_{k+1|k} - \boldsymbol{\beta}_{k+1|k}\hat{\boldsymbol{b}}_{k+1|k} \tag{27}$$

$$\tilde{\boldsymbol{P}}_{k+1|k}^{\boldsymbol{x}} = \boldsymbol{P}_{k+1|k}^{\boldsymbol{x}} - \boldsymbol{\beta}_{k+1|k}\boldsymbol{P}_{k+1|k}^{\boldsymbol{b}}\boldsymbol{\beta}_{k+1|k}^{\mathrm{T}} \tag{28}$$

For covariance matrices

$$\boldsymbol{P} = \begin{bmatrix} \boldsymbol{P}^{\boldsymbol{x}} & \boldsymbol{P}^{\boldsymbol{x}b} \\ \boldsymbol{P}^{\boldsymbol{b}x} & \boldsymbol{P}^{\boldsymbol{b}} \end{bmatrix}, \quad \sqrt{\boldsymbol{P}}$$

can be rewritten as

$$\sqrt{\boldsymbol{P}} = \begin{bmatrix} \sqrt{\boldsymbol{P}^{\boldsymbol{x}}} & \boldsymbol{0} \\ \boldsymbol{P}^{\boldsymbol{bx}}\left(\sqrt{\boldsymbol{P}^{\boldsymbol{x}}}^{\mathrm{T}}\right)^{-1} & \sqrt{\boldsymbol{P}^{\boldsymbol{b}} - \boldsymbol{P}^{\boldsymbol{bx}}\left(\boldsymbol{P}^{\boldsymbol{x}}\right)^{-1}\boldsymbol{P}^{\boldsymbol{xb}}} \end{bmatrix} \tag{29}$$

By substituting (29) into the original sigma points (11), the new sigma points can be written as

$$\begin{aligned} \boldsymbol{\chi}_k^{\boldsymbol{x}(0)} &= \hat{\boldsymbol{x}}_{k|k} \\ \boldsymbol{\chi}_k^{\boldsymbol{x}(i)} &= \begin{cases} \hat{\boldsymbol{x}}_{k|k} + \sqrt{L+\lambda}\sqrt{\boldsymbol{P}_{k|k}^{\boldsymbol{x}}}\boldsymbol{e}_i, \\ \qquad i = 1, \ldots, n \\ \boldsymbol{\chi}_k^{\boldsymbol{x}(0)}, \qquad i = n+1, \ldots, L \end{cases} \\ \boldsymbol{\chi}_k^{\boldsymbol{x}(i)} &= \begin{cases} \hat{\boldsymbol{x}}_{k|k} - \sqrt{L+\lambda}\sqrt{\boldsymbol{P}_{k|k}^{\boldsymbol{x}}}\boldsymbol{e}_{i-L}, \\ \qquad i = L+1, \ldots, L+n \\ \boldsymbol{\chi}_k^{\boldsymbol{x}(0)}, \quad i = L+n+1, \ldots, 2L \end{cases} \end{aligned} \tag{30}$$

and

$$\begin{aligned} \boldsymbol{\chi}_k^{\boldsymbol{b}(0)} &= \hat{\boldsymbol{b}}_{k|k} \\ \boldsymbol{\chi}_k^{\boldsymbol{b}(i)} &= \hat{\boldsymbol{b}}_{k|k} + \sqrt{L+\lambda}\boldsymbol{P}_{k|k}^{*}\boldsymbol{e}_i, \quad i = 1, \ldots, L \\ \boldsymbol{\chi}_k^{\boldsymbol{b}(i)} &= \hat{\boldsymbol{b}}_{k|k} - \sqrt{L+\lambda}\boldsymbol{P}_{k|k}^{*}\boldsymbol{e}_{i-L}, \quad i = L+1, \ldots, 2L \end{aligned} \tag{31}$$

where the ith element of $\boldsymbol{e}_i$ is 1 while the others are 0, and

$$\boldsymbol{P}_{k|k}^{*} = \left[\boldsymbol{P}_{k|k}^{\boldsymbol{bx}}\left(\sqrt{\boldsymbol{P}_{k|k}^{\boldsymbol{x}}}^{\mathrm{T}}\right)^{-1} \quad \sqrt{\boldsymbol{P}_{k|k}^{\boldsymbol{b}} - \boldsymbol{P}_{k|k}^{\boldsymbol{bx}}\left(\boldsymbol{P}_{k|k}^{\boldsymbol{x}}\right)^{-1}\boldsymbol{P}_{k|k}^{\boldsymbol{xb}}}\right]$$

Substituting (12) into (13), we can know

$$\boldsymbol{\chi}_{k+1|k}^{\boldsymbol{x}*}{}^{(i)} = \boldsymbol{f}_k\left(\boldsymbol{\chi}_k^{\boldsymbol{x}(i)}\right) + \boldsymbol{F}_k^{\mathrm{a}}\boldsymbol{\chi}_k^{\boldsymbol{b}(i)} \tag{32}$$

$$\boldsymbol{\chi}_{k+1|k}^{\boldsymbol{b}*}{}^{(i)} = \boldsymbol{\chi}_k^{\boldsymbol{b}(i)} \tag{33}$$

$$\hat{\boldsymbol{x}}_{k+1|k} = \sum_{i=0}^{2L} \omega_s^{(i)} \boldsymbol{\chi}_{k+1|k}^{\boldsymbol{x}*}{}^{(i)} \tag{34}$$

$$\hat{\boldsymbol{b}}_{k+1|k} = \sum_{i=0}^{2L} \omega_s^{(i)} \boldsymbol{\chi}_{k+1|k}^{\boldsymbol{b}*}{}^{(i)} \tag{35}$$

Expending (35) and (34) gives

$$\hat{\boldsymbol{b}}_{k+1|k} = \sum_{i=0}^{2L} \omega_s^{(i)} \boldsymbol{\chi}_{k+1|k}^{\boldsymbol{b}*}{}^{(i)} = \sum_{i=0}^{2L} \omega_s^{(i)} \boldsymbol{\chi}_k^{\boldsymbol{b}(i)} = \hat{\boldsymbol{b}}_{k|k} \tag{36}$$

and then we can compute (34) further

$$\begin{aligned} \hat{\boldsymbol{x}}_{k+1|k} &= \sum_{i=0}^{2L} \omega_s^{(i)} \left[\boldsymbol{f}_k\left(\boldsymbol{\chi}_k^{\boldsymbol{x}(i)}\right) + \boldsymbol{F}_k^{\mathrm{a}}\boldsymbol{\chi}_k^{\boldsymbol{b}(i)}\right] \\ &= \sum_{i=0}^{2L} \omega_s^{(i)} \boldsymbol{f}_k\left(\boldsymbol{\chi}_k^{\boldsymbol{x}(i)}\right) + \boldsymbol{F}_k^{\mathrm{a}}\hat{\boldsymbol{b}}_{k|k} \\ &= \boldsymbol{m}_k + \boldsymbol{F}_k^{\mathrm{a}}\hat{\boldsymbol{b}}_{k|k} \end{aligned} \tag{37}$$

with the definition

$$\boldsymbol{m}_k = \sum_{i=0}^{2n} \omega_s^{\boldsymbol{x}(i)} \boldsymbol{f}_k\left(\boldsymbol{\chi}_k^{\boldsymbol{x}(i)}\right) \tag{38}$$

Computing (14) blockwise obtains

$$\begin{aligned} \boldsymbol{P}_{k+1|k}^{\boldsymbol{x}} &= \boldsymbol{W}_k^{\boldsymbol{x}} \\ &\quad + \sum_{i=0}^{2L} \omega_c^{(i)}\left(\boldsymbol{\chi}_{k+1|k}^{\boldsymbol{x}*}{}^{(i)} - \hat{\boldsymbol{x}}_{k+1|k}\right)\left(\boldsymbol{\chi}_{k+1|k}^{\boldsymbol{x}*}{}^{(i)} - \hat{\boldsymbol{x}}_{k+1|k}\right)^{\mathrm{T}} \end{aligned} \tag{39}$$

$$\begin{aligned} \boldsymbol{P}_{k+1|k}^{\boldsymbol{b}} &= \boldsymbol{W}_k^{\boldsymbol{b}} \\ &\quad + \sum_{i=0}^{2L} \omega_c^{(i)}\left(\boldsymbol{\chi}_k^{\boldsymbol{b}(i)} - \hat{\boldsymbol{b}}_{k|k}\right)\left(\boldsymbol{\chi}_k^{\boldsymbol{b}(i)} - \hat{\boldsymbol{b}}_{k|k}\right)^{\mathrm{T}} \\ &= \boldsymbol{W}_k^{\boldsymbol{b}} + \boldsymbol{P}_{k|k}^{*}\boldsymbol{P}_{k|k}^{*}{}^{\mathrm{T}} \\ &= \boldsymbol{W}_k^{\boldsymbol{b}} + \boldsymbol{P}_{k|k}^{\boldsymbol{b}} \end{aligned} \tag{40}$$

$$\begin{aligned} &\boldsymbol{P}_{k+1|k}^{\boldsymbol{xb}} \\ &= \sum_{i=0}^{2L} \omega_c^{(i)}\left(\boldsymbol{\chi}_{k+1|k}^{\boldsymbol{x}*}{}^{(i)} - \hat{\boldsymbol{x}}_{k+1|k}\right)\left(\boldsymbol{\chi}_{k+1|k}^{\boldsymbol{b}*}{}^{(i)} - \hat{\boldsymbol{b}}_{k+1|k}\right)^{\mathrm{T}} \end{aligned} \tag{41}$$

Substituting (40) and (41) into (24) yields

$$\begin{aligned} &\boldsymbol{\beta}_{k+1|k} \\ &= \left[\sum_{i=0}^{2L} \omega_c^{(i)}\left(\boldsymbol{\chi}_{k+1|k}^{x}{}^{(i)} - \hat{\boldsymbol{x}}_{k+1|k}\right)\left(\boldsymbol{\chi}_k^{\boldsymbol{b}(i)} - \hat{\boldsymbol{b}}_{k|k}\right)^{\mathrm{T}}\right] \\ &\quad \times \left(\boldsymbol{P}_{k|k}^{\boldsymbol{b}} + \boldsymbol{W}_k^{\boldsymbol{b}}\right)^{-1} \\ &= \frac{1}{2\sqrt{3\alpha}}\left[\sum_{i=1}^{L}\left(\boldsymbol{f}_k\left(\boldsymbol{\chi}_k^{\boldsymbol{x}(i)}\right) - \boldsymbol{f}_k\left(\boldsymbol{\chi}_k^{\boldsymbol{x}(i+L)}\right)\right)\left(\boldsymbol{P}_{k|k}^{*}\boldsymbol{e}_i\right)^{\mathrm{T}}\right] \\ &\quad \times \left(\boldsymbol{P}_{k|k}^{\boldsymbol{b}} + \boldsymbol{W}_k^{\boldsymbol{b}}\right)^{-1} \\ &\quad + \boldsymbol{F}_k^{\mathrm{a}}\boldsymbol{P}_{k|k}^{*}\boldsymbol{P}_{k|k}^{*}{}^{\mathrm{T}}\left(\boldsymbol{P}_{k|k}^{\boldsymbol{b}} + \boldsymbol{W}_k^{\boldsymbol{b}}\right)^{-1} \\ &= \boldsymbol{R}_k\boldsymbol{P}_{k|k}^{\boldsymbol{b}}\left(\boldsymbol{P}_{k|k}^{\boldsymbol{b}} + \boldsymbol{W}_k^{\boldsymbol{b}}\right)^{-1} \end{aligned} \tag{42}$$

with the definition

$$\boldsymbol{R}_k = \boldsymbol{M}_k\boldsymbol{\beta}_{k|k} + \boldsymbol{F}_k^{\mathrm{a}} \tag{43}$$

where

$$\begin{aligned} \boldsymbol{M}_k &= \frac{1}{2\sqrt{3\alpha}} \\ &\quad \times \left\{\sum_{i=1}^{n}\left[\boldsymbol{f}_k\left(\boldsymbol{\chi}_k^{\boldsymbol{x}(i)}\right) - \boldsymbol{f}_k\left(\boldsymbol{\chi}_k^{\boldsymbol{x}(i+L)}\right)\right]\boldsymbol{e}_i^{\mathrm{T}}\right\}\left(\sqrt{\boldsymbol{P}_{k|k}^{\boldsymbol{x}}}\right)^{-1} \end{aligned} \tag{44}$$

Compute (39)

$$\begin{aligned} &\boldsymbol{P}_{k+1|k}^{\boldsymbol{x}} \\ &= \sum_{i=0}^{2n} \omega_c^{\boldsymbol{x}(i)}\left[\boldsymbol{f}_k\left(\boldsymbol{\chi}_k^{\boldsymbol{x}(i)}\right) - \boldsymbol{m}_k\right]\left[\boldsymbol{f}_k\left(\boldsymbol{\chi}_k^{\boldsymbol{x}(i)}\right) - \boldsymbol{m}_k\right]^{\mathrm{T}} \\ &\quad + \boldsymbol{M}_k\boldsymbol{\beta}_{k|k}\boldsymbol{P}_{k|k}^{\boldsymbol{b}}\boldsymbol{F}_k^{\mathrm{a}\mathrm{T}} + \boldsymbol{F}_k^{\mathrm{a}}\boldsymbol{P}_{k|k}^{\boldsymbol{b}}\left(\boldsymbol{M}_k\boldsymbol{\beta}_{k|k}\right)^{\mathrm{T}} \\ &\quad + \boldsymbol{F}_k^{\mathrm{a}}\boldsymbol{P}_{k|k}^{\boldsymbol{b}}\boldsymbol{F}_k^{\mathrm{a}\mathrm{T}} + \boldsymbol{W}_k^{x} \\ &= \sum_{i=0}^{2n} \omega_c^{\boldsymbol{x}(i)}\left[\boldsymbol{f}_k\left(\boldsymbol{\chi}_k^{\boldsymbol{x}(i)}\right) - \boldsymbol{m}_k\right]\left[\boldsymbol{f}_k\left(\boldsymbol{\chi}_k^{\boldsymbol{x}(i)}\right) - \boldsymbol{m}_k\right]^{\mathrm{T}} \\ &\quad - \boldsymbol{M}_k\boldsymbol{\beta}_{k|k}\boldsymbol{P}_{k|k}^{\boldsymbol{b}}\boldsymbol{\beta}_{k|k}^{\mathrm{T}}\boldsymbol{M}_k^{\mathrm{T}} + \boldsymbol{R}_k\boldsymbol{P}_{k|k}^{\boldsymbol{b}}\boldsymbol{R}_k^{\mathrm{T}} + \boldsymbol{W}_k^{\boldsymbol{x}} \end{aligned} \tag{45}$$

With (15) and (29), the sigma points and the corresponding weights could be computed as follows:

$$
\begin{aligned}
\boldsymbol{\chi}^{\boldsymbol{x}}_{k+1|k}{}^{(0)} &= \hat{\boldsymbol{x}}_{k+1|k} \\
\boldsymbol{\chi}^{\boldsymbol{x}}_{k+1|k}{}^{(i)} &= \begin{cases} \hat{\boldsymbol{x}}_{k+1|k} + \sqrt{(L+\lambda)\boldsymbol{P}^{\boldsymbol{x}}_{k+1|k}}\boldsymbol{e}_i, \\ \qquad i = 1, \ldots, n \\ \hat{\boldsymbol{x}}_{k+1|k}, \quad i = n+1, \ldots, L \end{cases} \\
\boldsymbol{\chi}^{\boldsymbol{x}}_{k+1|k}{}^{(i)} &= \begin{cases} \hat{\boldsymbol{x}}_{k+1|k} - \sqrt{(L+\lambda)\boldsymbol{P}^{\boldsymbol{x}}_{k+1|k}}\boldsymbol{e}_{i-L}, \\ \qquad i = L+1, \ldots, L+n \\ \hat{\boldsymbol{x}}_{k+1|k}, \quad i = L+n, \ldots, 2L \end{cases}
\end{aligned} \tag{46}
$$

and

$$
\begin{aligned}
\boldsymbol{\chi}^{\boldsymbol{b}}_{k+1|k}{}^{(0)} &= \hat{\boldsymbol{b}}_{k+1|k} \\
\boldsymbol{\chi}^{\boldsymbol{b}}_{k+1|k}{}^{(i)} &= \hat{\boldsymbol{b}}_{k+1|k} \pm \sqrt{L+\lambda}\boldsymbol{P}^{*}_{k+1|k}\boldsymbol{e}_i, \quad i = 1, \ldots, L
\end{aligned} \tag{47}
$$

where

$$
\begin{aligned}
\boldsymbol{P}^{*}_{k+1|k} &= \begin{bmatrix} \boldsymbol{P}^{*1} & \boldsymbol{P}^{*2} \end{bmatrix} \\
\boldsymbol{P}^{*1} &= \boldsymbol{P}^{\boldsymbol{bx}}_{k+1|k}\left(\sqrt{\boldsymbol{P}^{\boldsymbol{x}}_{k+1|k}}^{\mathrm{T}}\right)^{-1} \\
\boldsymbol{P}^{*2} &= \sqrt{\boldsymbol{P}^{\boldsymbol{b}}_{k+1|k} - \boldsymbol{P}^{\boldsymbol{bx}}_{k+1|k}\left(\boldsymbol{P}^{\boldsymbol{x}}_{k+1|k}\right)^{-1}\boldsymbol{P}^{\boldsymbol{xb}}_{k+1|k}}
\end{aligned}
$$

The one-step prediction equation of the measurement in (16) can be rewritten as

$$
\boldsymbol{y}_{k+1|k}{}^{(i)} = \boldsymbol{h}_{k+1}\left(\boldsymbol{\chi}^{\boldsymbol{x}}_{k+1|k}{}^{(i)}\right) + \boldsymbol{F}^{\mathrm{s}}_{k+1}\boldsymbol{\chi}^{\boldsymbol{b}}_{k+1|k}{}^{(i)} \tag{48}
$$

where $i = 0, 1, \ldots, 2L$. Then the one-step prediction of the measurement at the (k+1) step in (17) can be computed as follows:

$$
\begin{aligned}
\hat{\boldsymbol{y}}_{k+1|k} &= \sum_{i=0}^{2L} \omega_s{}^{(i)}\boldsymbol{h}_{k+1}\left(\boldsymbol{\chi}^{\boldsymbol{x}}_{k+1|k}{}^{(i)}\right) \\
&\quad + \boldsymbol{F}^{\mathrm{s}}_{k+1}\sum_{i=0}^{2L} \omega_s{}^{(i)}\boldsymbol{\chi}^{\boldsymbol{b}}_{k+1|k}{}^{(i)} \\
&= \boldsymbol{n}_{k+1} + \boldsymbol{F}^{\mathrm{s}}_{k+1}\hat{\boldsymbol{b}}_{k+1|k}
\end{aligned} \tag{49}
$$

with the definition

$$
\boldsymbol{n}_{k+1} = \sum_{i=0}^{2n} \omega^{\boldsymbol{x}}_s{}^{(i)}\boldsymbol{h}_{k+1}\left(\boldsymbol{\chi}^{\boldsymbol{x}}_{k+1|k}{}^{(i)}\right) \tag{50}
$$

and therefore with the definition $\boldsymbol{\gamma}^{(i)}_{k+1} = \boldsymbol{h}_{k+1}\left(\boldsymbol{\chi}^{\boldsymbol{x}}_{k+1|k}{}^{(i)}\right) - \boldsymbol{n}_{k+1}$, $\boldsymbol{P}^{\boldsymbol{yy}}_{k+1|k}$ in (18) could be calculated

$$
\begin{aligned}
\boldsymbol{P}^{\boldsymbol{yy}}_{k+1|k} &= \sum_{i=0}^{2n} \omega^{\boldsymbol{x}}_c{}^{(i)}\boldsymbol{\gamma}^{(i)}_{k+1}\boldsymbol{\gamma}^{(i)\ \mathrm{T}}_{k+1} + \boldsymbol{N}_{k+1}\boldsymbol{\beta}_{k+1|k}\boldsymbol{P}^{\boldsymbol{b}}_{k+1|k}\boldsymbol{F}^{\mathrm{sT}}_{k+1} \\
&\quad + \boldsymbol{F}^{\mathrm{s}}_{k+1}\boldsymbol{P}^{\boldsymbol{b}}_{k+1|k}\boldsymbol{\beta}^{\mathrm{T}}_{k+1|k}\boldsymbol{N}^{\mathrm{T}}_{k+1} + \boldsymbol{F}^{\mathrm{s}}_{k+1}\boldsymbol{P}^{\boldsymbol{b}}_{k+1|k}\boldsymbol{F}^{\mathrm{sT}}_{k+1} + \boldsymbol{V}_k \\
&= \sum_{i=0}^{2n} \omega^{\boldsymbol{x}}_c{}^{(i)}\boldsymbol{\gamma}^{(i)}_{k+1}\boldsymbol{\gamma}^{(i)\ \mathrm{T}}_{k+1} \\
&\quad - \boldsymbol{N}_{k+1}\boldsymbol{\beta}_{k+1|k}\boldsymbol{P}^{\boldsymbol{b}}_{k+1|k}\boldsymbol{\beta}^{\mathrm{T}}_{k+1|k}\boldsymbol{N}^{\mathrm{T}}_{k+1} \\
&\quad + \boldsymbol{H}_{k+1|k}\boldsymbol{P}^{\boldsymbol{b}}_{k+1|k}\boldsymbol{H}^{\mathrm{T}}_{k+1|k} + \boldsymbol{V}_k
\end{aligned} \tag{51}
$$

with the definition

$$
\boldsymbol{H}_{k+1|k} = \boldsymbol{N}_{k+1}\boldsymbol{\beta}_{k+1|k} + \boldsymbol{F}^{\mathrm{s}}_{k+1} \tag{52}
$$

where

$$
\begin{aligned}
\boldsymbol{N}_{k+1} &= \frac{1}{2\sqrt{3\alpha}} \\
&\quad \times \left\{ \sum_{i=1}^{n} \left[\boldsymbol{h}_{k+1}\left(\boldsymbol{\chi}^{\boldsymbol{x}}_{k+1|k}{}^{(i)}\right) - \boldsymbol{h}_{k+1}\left(\boldsymbol{\chi}^{\boldsymbol{x}}_{k+1|k}{}^{(i+L)}\right)\right]\boldsymbol{e}^{\mathrm{T}}_i \right\} \\
&\quad \times \left(\sqrt{\boldsymbol{P}^{\boldsymbol{x}}_{k+1|k}}\right)^{-1}
\end{aligned} \tag{53}
$$

For convenience, when expending $\boldsymbol{P}^{\boldsymbol{Xy}}_{k+1|k}$ in (19), $\boldsymbol{P}^{\boldsymbol{yy}}_{k+1|k}$ in (51) is first approximated, and then replaced by the accurate equation in the further derivation process. Define that

$$
\boldsymbol{Q} = \sum_{i=0}^{2n} \omega^{\boldsymbol{x}}_c{}^{(i)}\boldsymbol{\gamma}^{(i)}_{k+1}\boldsymbol{\gamma}^{(i)\ \mathrm{T}}_{k+1}
$$

the approximation of $\boldsymbol{Q}$ is given as follows. For the continuous function $\boldsymbol{h}(\cdot)$ which is retained up to the first-order term in Taylor series expansion, we can also define that $\boldsymbol{h}_{k+1}\left(\hat{\boldsymbol{x}}_{k+1|k}\right) \simeq \boldsymbol{C}\hat{\boldsymbol{x}}_{k+1|k}$, where $\partial\boldsymbol{h}/\partial\boldsymbol{x}|_{\boldsymbol{x}=\hat{\boldsymbol{x}}_{\boldsymbol{k+1|k}}} = \boldsymbol{C}$, and therefore

$$
\boldsymbol{Q} \simeq \boldsymbol{N}_{k+1}\boldsymbol{P}^{\boldsymbol{x}}_{k+1|k}\boldsymbol{N}^{\mathrm{T}}_{k+1} \tag{54}
$$

Thus, $\boldsymbol{P}^{\boldsymbol{xy}}_{k+1|k}$ and $\boldsymbol{P}^{\boldsymbol{by}}_{k+1|k}$ can be computed

$$
\begin{aligned}
\boldsymbol{P}^{\boldsymbol{x}y}_{k+1|k} &= \sum_{i=1}^{2L} \omega_c{}^{(i)}\left(\boldsymbol{\chi}^{\boldsymbol{x}}_{k+1|k}{}^{(i)} - \hat{\boldsymbol{x}}_{k+1|k}\right)\left(\boldsymbol{y}_{k+1|k}{}^{(i)} - \hat{\boldsymbol{y}}_{k+1|k}\right)^{\mathrm{T}} \\
&= \frac{1}{2\sqrt{3\alpha}} \\
&\quad \times \sum_{i=1}^{n} \sqrt{\boldsymbol{P}^{\boldsymbol{x}}_{k+1|k}}\boldsymbol{e}_i\left[\boldsymbol{h}_k\left(\boldsymbol{\chi}^{\boldsymbol{x}}_{k+1|k}{}^{(i)}\right) - \boldsymbol{h}_k\left(\boldsymbol{\chi}^{\boldsymbol{x}}_{k+1|k}{}^{(i+L)}\right)\right]^{\mathrm{T}} \\
&\quad + \frac{1}{2\sqrt{3\alpha}}\sum_{i=1}^{n} \sqrt{\boldsymbol{P}^{\boldsymbol{x}}_{k+1|k}}\boldsymbol{e}_i\left(\boldsymbol{\chi}^{\boldsymbol{b}}_{k+1|k}{}^{(i)} - \boldsymbol{\chi}^{\boldsymbol{b}}_{k+1|k}{}^{(i+L)}\right)^{\mathrm{T}}\boldsymbol{F}^{\mathrm{sT}}_k \\
&\simeq \boldsymbol{P}^{\boldsymbol{x}}_{k+1|k}\boldsymbol{N}^{\mathrm{T}}_{k+1} + \boldsymbol{\beta}_{k+1|k}\boldsymbol{P}^{\boldsymbol{b}}_{k+1|k}\boldsymbol{F}^{\mathrm{sT}}_k \\
&= \tilde{\boldsymbol{P}}^{\boldsymbol{x}}_{k+1|k}\boldsymbol{N}^{\mathrm{T}}_{k+1} + \boldsymbol{\beta}_{k+1|k}\boldsymbol{P}^{\boldsymbol{b}}_{k+1|k}\boldsymbol{H}^{\mathrm{T}}_{k+1|k}
\end{aligned} \tag{55}
$$

$$
\begin{aligned}
\boldsymbol{P}^{\boldsymbol{b}y}_{k+1|k} &= \sum_{i=0}^{2L} \omega_c{}^{(i)}\left(\boldsymbol{\chi}^{\boldsymbol{b}}_{k+1|k}{}^{(i)} - \hat{\boldsymbol{b}}_{k+1|k}\right)\left(\boldsymbol{y}_{k+1|k}{}^{(i)} - \hat{\boldsymbol{y}}_{k+1|k}\right)^{\mathrm{T}} \\
&= \boldsymbol{P}^{\boldsymbol{b}}_{k+1|k}\boldsymbol{\beta}^{\mathrm{T}}_{k+1|k}\boldsymbol{N}^{\mathrm{T}}_{k+1} + \boldsymbol{P}^{\boldsymbol{b}}_{k+1|k}\boldsymbol{F}^{\mathrm{sT}}_{k+1} \\
&= \boldsymbol{P}^{\boldsymbol{b}}_{k+1|k}\boldsymbol{H}^{\mathrm{T}}_{k+1|k}
\end{aligned} \tag{56}
$$

Then substituting (56) into (55) yields

$$
\boldsymbol{P}^{\boldsymbol{x}y}_{k+1|k} = \tilde{\boldsymbol{P}}^{\boldsymbol{x}}_{k+1|k}\boldsymbol{N}^{\mathrm{T}}_{k+1} + \boldsymbol{\beta}_{k+1|k}\boldsymbol{P}^{\boldsymbol{b}y}_{k+1|k} \tag{57}
$$

Compute (22)

$$
\begin{aligned}
\boldsymbol{P}_{k+1|k+1} &= \boldsymbol{P}_{k+1|k} - \begin{bmatrix} \tilde{\boldsymbol{P}}^{\boldsymbol{x}}_{k+1|k}\boldsymbol{N}^{\mathrm{T}}_{k+1} + \boldsymbol{\beta}_{k+1|k}\boldsymbol{P}^{\boldsymbol{b}}_{k+1|k}\boldsymbol{H}^{\mathrm{T}}_{k+1|k} \\ \boldsymbol{P}^{\boldsymbol{b}}_{k+1|k}\boldsymbol{H}^{\mathrm{T}}_{k+1|k} \end{bmatrix} \\
&\quad \times \left(\boldsymbol{P}^{\boldsymbol{yy}}_{k+1|k}\right)^{-1}\begin{bmatrix} \tilde{\boldsymbol{P}}^{\boldsymbol{x}}_{k+1|k}\boldsymbol{N}^{\mathrm{T}}_{k+1} + \boldsymbol{\beta}_{k+1|k}\boldsymbol{P}^{\boldsymbol{b}}_{k+1|k}\boldsymbol{H}^{\mathrm{T}}_{k+1|k} \\ \boldsymbol{P}^{\boldsymbol{b}}_{k+1|k}\boldsymbol{H}^{\mathrm{T}}_{k+1|k} \end{bmatrix}^{\mathrm{T}} \\
&= \boldsymbol{P}_{k+1|k} - \boldsymbol{P}_{k+1|k}\begin{bmatrix} \boldsymbol{N}^{\mathrm{T}}_{k+1} \\ \boldsymbol{F}^{\mathrm{sT}}_{k+1} \end{bmatrix}\left(\boldsymbol{P}^{\boldsymbol{yy}}_{k+1|k}\right)^{-1}\begin{bmatrix} \boldsymbol{N}^{\mathrm{T}}_{k+1} \\ \boldsymbol{F}^{\mathrm{sT}}_{k+1} \end{bmatrix}^{\mathrm{T}}\boldsymbol{P}_{k+1|k}
\end{aligned} \tag{58}
$$

As $\boldsymbol{P}^{\boldsymbol{yy}}_{k+1|k}$ in (51) can be approximatively rewritten as

$$\begin{aligned}\boldsymbol{P}^{\boldsymbol{yy}}_{k+1|k} &= \boldsymbol{N}_{k+1}\boldsymbol{P}^{\boldsymbol{x}}_{k+1|k}\boldsymbol{N}^{\mathrm{T}}_{k+1} - \boldsymbol{N}_{k+1}\boldsymbol{\beta}_{k+1|k}\boldsymbol{P}^{\boldsymbol{b}}_{k+1|k}\boldsymbol{\beta}^{\mathrm{T}}_{k+1|k}\boldsymbol{N}^{\mathrm{T}}_{k+1} \\ &\quad +(\boldsymbol{N}_{k+1}\boldsymbol{\beta}_{k+1|k}+\boldsymbol{F}^{\mathrm{s}}_{k+1})\boldsymbol{P}^{\boldsymbol{b}}_{k+1|k}(\boldsymbol{C}_{k+1}\boldsymbol{\beta}_{k+1|k}+\boldsymbol{F}^{\mathrm{s}}_{k+1})^{\mathrm{T}} \\ &\quad +\boldsymbol{V}_k \\ &= \begin{bmatrix}\boldsymbol{N}_{k+1} & \boldsymbol{F}^{\mathrm{s}}_{k+1}\end{bmatrix}\boldsymbol{P}_{k+1|k}\begin{bmatrix}\boldsymbol{N}^{\mathrm{T}}_{k+1} \\ \boldsymbol{F}^{\mathrm{sT}}_{k+1}\end{bmatrix}+\boldsymbol{V}_k\end{aligned} \tag{59}$$

we can compute $\boldsymbol{P}_{k+1|k+1}$ in (58) further

$$\begin{aligned}&\boldsymbol{P}_{k+1|k+1} \\ &= \left\{\begin{bmatrix}\boldsymbol{N}^{\mathrm{T}}_{k+1} \\ \boldsymbol{F}^{\mathrm{sT}}_{k+1}\end{bmatrix}\boldsymbol{V}^{-1}_k\begin{bmatrix}\boldsymbol{N}_{k+1} & \boldsymbol{F}^{\mathrm{s}}_{k+1}\end{bmatrix}+(\boldsymbol{P}_{k+1|k})^{-1}\right\}^{-1} \\ &= \begin{bmatrix}\boldsymbol{P}_1 & \boldsymbol{P}_2 \\ \boldsymbol{P}_3 & \boldsymbol{P}_4\end{bmatrix}^{-1}\end{aligned} \tag{60}$$

where

$$\boldsymbol{P}_1 = \boldsymbol{N}^{\mathrm{T}}_{k+1}\boldsymbol{V}^{-1}_k\boldsymbol{N}_{k+1}+\left(\tilde{\boldsymbol{P}}^{\boldsymbol{x}}_{k+1|k}\right)^{-1} \tag{61}$$

$$\boldsymbol{P}_2 = \boldsymbol{P}_3{}^{\mathrm{T}} = \boldsymbol{N}_{k+1}\boldsymbol{V}^{-1}_k\boldsymbol{F}^{\mathrm{s}}_{k+1}-\left(\tilde{\boldsymbol{P}}^{\boldsymbol{x}}_{k+1|k}\right)^{-1}\boldsymbol{\beta}_{k+1|k} \tag{62}$$

$$\boldsymbol{P}_4 = \boldsymbol{F}^{\mathrm{sT}}_{k+1}\boldsymbol{V}^{-1}_k\boldsymbol{F}^{\mathrm{s}}_{k+1}+\left(\boldsymbol{P}^{\boldsymbol{b}}_{k+1|k}\right)^{-1} \tag{63}$$

As the matrix $\boldsymbol{P}_{k+1|k+1}$ in (60) is partitioned into four blocks, it can be inverted blockwise and we can get

$$\boldsymbol{P}^{\boldsymbol{b}}_{k+1|k+1} = \left(\boldsymbol{P}_4-\boldsymbol{P}_3\boldsymbol{P}^{-1}_1\boldsymbol{P}_2\right)^{-1} \tag{64a}$$

$$\boldsymbol{\beta}_{k+1|k+1} = \boldsymbol{P}^{\boldsymbol{xb}}_{k+1|k+1}\left(\boldsymbol{P}^{\boldsymbol{b}}_{k+1|k+1}\right)^{-1} = -\boldsymbol{P}^{-1}_1\boldsymbol{P}_2 \tag{64b}$$

$$\tilde{\boldsymbol{P}}^{\boldsymbol{x}}_{k+1|k+1} = \boldsymbol{P}^{-1}_1 \tag{64c}$$

Compute $\boldsymbol{K}_{k+1}$ in (20)

$$\begin{aligned}\boldsymbol{K}_{k+1} &= \begin{bmatrix}\boldsymbol{K}^{\boldsymbol{x}}_{k+1} \\ \boldsymbol{K}^{\boldsymbol{b}}_{k+1}\end{bmatrix} = \begin{bmatrix}\boldsymbol{P}^{\boldsymbol{xy}}_{k+1|k} \\ \boldsymbol{P}^{\boldsymbol{by}}_{k+1|k}\end{bmatrix}\left(\boldsymbol{P}^{\boldsymbol{yy}}_{k+1|k}\right)^{-1} \\ &= \boldsymbol{P}_{k+1|k}\begin{bmatrix}\boldsymbol{N}^{\mathrm{T}}_{k+1} \\ \boldsymbol{F}^{\mathrm{sT}}_{k+1}\end{bmatrix} \\ &\quad \times\left(\begin{bmatrix}\boldsymbol{N}_{k+1} & \boldsymbol{F}^{\mathrm{s}}_{k+1}\end{bmatrix}\boldsymbol{P}_{k+1|k}\begin{bmatrix}\boldsymbol{N}^{\mathrm{T}}_{k+1} \\ \boldsymbol{F}^{\mathrm{sT}}_{k+1}\end{bmatrix}+\boldsymbol{V}_k\right)^{-1} \\ &= \boldsymbol{P}_{k+1|k+1}\begin{bmatrix}\boldsymbol{N}^{\mathrm{T}}_{k+1} \\ \boldsymbol{F}^{\mathrm{sT}}_{k+1}\end{bmatrix}\boldsymbol{V}^{-1}_k \\ &= \begin{bmatrix}\tilde{\boldsymbol{P}}^{\boldsymbol{x}}_{k+1|k+1}\boldsymbol{N}^{\mathrm{T}}_{k+1}+\boldsymbol{\beta}_{k+1|k+1}\boldsymbol{P}^{\boldsymbol{b}}_{k+1|k+1}\boldsymbol{H}^{\mathrm{T}}_{k+1|k+1} \\ \boldsymbol{P}^{\boldsymbol{b}}_{k+1|k+1}\boldsymbol{H}^{\mathrm{T}}_{k+1|k+1}\end{bmatrix}\boldsymbol{V}^{-1}_k\end{aligned} \tag{65}$$

where

$$\boldsymbol{P}^{\boldsymbol{x}}_{k+1|k+1} = \tilde{\boldsymbol{P}}^{\boldsymbol{x}}_{k+1|k+1}+\boldsymbol{\beta}_{k+1|k+1}\boldsymbol{P}^{\boldsymbol{b}}_{k+1|k+1}\boldsymbol{\beta}^{\mathrm{T}}_{k+1|k+1} \tag{66}$$

i.e.

$$\begin{aligned}\boldsymbol{K}^{\boldsymbol{x}}_{k+1} &= \left(\tilde{\boldsymbol{P}}^{\boldsymbol{x}}_{k+1|k+1}\boldsymbol{N}^{\mathrm{T}}_{k+1}+\boldsymbol{\beta}_{k+1|k+1}\boldsymbol{P}^{\boldsymbol{b}}_{k+1|k+1}\boldsymbol{H}^{\mathrm{T}}_{k+1|k+1}\right)\boldsymbol{V}^{-1}_k \\ &= \tilde{\boldsymbol{P}}^{\boldsymbol{x}}_{k+1|k+1}\boldsymbol{N}^{\mathrm{T}}_{k+1}\boldsymbol{V}^{-1}_k+\boldsymbol{\beta}_{k+1|k+1}\boldsymbol{K}^{\boldsymbol{b}}_{k+1}\end{aligned} \tag{67}$$

Thus, $\tilde{\boldsymbol{K}}^{\boldsymbol{x}}_{k+1}$ can be defined and computed as follows:

$$\begin{aligned}\tilde{\boldsymbol{K}}^{\boldsymbol{x}}_{k+1} &= \tilde{\boldsymbol{P}}^{\boldsymbol{x}}_{k+1|k+1}\boldsymbol{N}^{\mathrm{T}}_{k+1}\boldsymbol{V}^{-1}_k \\ &= \left[\boldsymbol{N}^{\mathrm{T}}_{k+1}\boldsymbol{V}^{-1}_k\boldsymbol{N}_{k+1}+\left(\tilde{\boldsymbol{P}}^{x}_{k+1|k}\right)^{-1}\right]^{-1}\boldsymbol{N}^{\mathrm{T}}_{k+1}\boldsymbol{V}^{-1}_k \\ &= \tilde{\boldsymbol{P}}^{x}_{k+1|k}\boldsymbol{N}^{\mathrm{T}}_{k+1}\left(\boldsymbol{N}_{k+1}\tilde{\boldsymbol{P}}^{x}_{k+1|k}\boldsymbol{N}^{\mathrm{T}}_{k+1}+\boldsymbol{V}_k\right)^{-1}\end{aligned} \tag{68}$$

Therefore, $\tilde{\boldsymbol{P}}^{\boldsymbol{x}}_{k+1|k+1}$ in (64c) can be calculated with (68)

$$\begin{aligned}&\tilde{\boldsymbol{P}}^{\boldsymbol{x}}_{k+1|k+1} \\ &= \tilde{\boldsymbol{P}}^{\boldsymbol{x}}_{k+1|k} \\ &\quad -\tilde{\boldsymbol{P}}^{\boldsymbol{x}}_{k+1|k}\boldsymbol{N}^{\mathrm{T}}_{k+1}\left(\boldsymbol{N}_{k+1}\tilde{\boldsymbol{P}}^{\boldsymbol{x}}_{k+1|k}\boldsymbol{N}^{\mathrm{T}}_{k+1}+\boldsymbol{V}_k\right)^{-1}\boldsymbol{N}_{k+1}\tilde{\boldsymbol{P}}^{\boldsymbol{x}}_{k+1|k} \\ &= \tilde{\boldsymbol{P}}^{\boldsymbol{x}}_{k+1|k}-\tilde{\boldsymbol{K}}^{\boldsymbol{x}}_{k+1}\tilde{\boldsymbol{P}}^{\boldsymbol{yy}}_{k+1|k}\tilde{\boldsymbol{K}}^{\boldsymbol{x}\mathrm{T}}_{k+1}\end{aligned} \tag{69}$$

with the definition

$$\begin{aligned}\tilde{\boldsymbol{P}}^{\boldsymbol{yy}}_{k+1|k} &= \boldsymbol{N}_{k+1}\tilde{\boldsymbol{P}}^{\boldsymbol{x}}_{k+1|k}\boldsymbol{N}^{\mathrm{T}}_{k+1}+\boldsymbol{V}_k \\ &= \sum_{i=0}^{2n}\omega^{\boldsymbol{x}(i)}_c\boldsymbol{\gamma}^{(i)}_{k+1}\boldsymbol{\gamma}^{(i)\ \mathrm{T}}_{k+1} \\ &\quad -\boldsymbol{N}_{k+1}\boldsymbol{\beta}_{k+1|k}\boldsymbol{P}^{\boldsymbol{b}}_{k+1|k}\boldsymbol{\beta}^{\mathrm{T}}_{k+1|k}\boldsymbol{N}^{\mathrm{T}}_{k+1}+\boldsymbol{V}_k\end{aligned} \tag{70}$$

where the approximation is replaced by the accurate formula in (54). Thereby $\boldsymbol{P}^{\boldsymbol{yy}}_{k+1|k}$ in (51) is rewritten as

$$\boldsymbol{P}^{\boldsymbol{yy}}_{k+1|k} = \tilde{\boldsymbol{P}}^{\boldsymbol{yy}}_{k+1|k}+\boldsymbol{H}_{k+1|k}\boldsymbol{P}^{b}_{k+1|k}\boldsymbol{H}^{\mathrm{T}}_{k+1|k} \tag{71}$$

Also, from (65), $\boldsymbol{K}^{\boldsymbol{b}}_{k+1}$ can be written in another form by substituting (56) into it

$$\begin{aligned}\boldsymbol{K}^{\boldsymbol{b}}_{k+1} &= \boldsymbol{P}^{\boldsymbol{by}}_{k+1|k}\left(\boldsymbol{P}^{\boldsymbol{yy}}_{k+1|k}\right)^{-1} \\ &= \boldsymbol{P}^{\boldsymbol{b}}_{k+1|k}\boldsymbol{H}^{\mathrm{T}}_{k+1|k}\left(\boldsymbol{P}^{\boldsymbol{yy}}_{k+1|k}\right)^{-1}\end{aligned} \tag{72}$$

From (21), $\hat{\boldsymbol{x}}_{k+1|k+1}$ and $\hat{\boldsymbol{b}}_{k+1|k+1}$ could be computed

$$\begin{aligned}\hat{\boldsymbol{x}}_{k+1|k+1} &= \hat{\boldsymbol{x}}_{k+1|k}+\boldsymbol{K}^{\boldsymbol{x}}_{k+1}\left(\boldsymbol{y}_{k+1}-\hat{\boldsymbol{y}}_{k+1|k}\right) \\ &= \tilde{\boldsymbol{x}}_{k+1|k}+\boldsymbol{\beta}_{k+1|k}\hat{\boldsymbol{b}}_{k+1|k}+\tilde{\boldsymbol{K}}^{\boldsymbol{x}}_{k+1}\left(\boldsymbol{y}_{k+1}-\hat{\boldsymbol{y}}_{k+1|k}\right) \\ &\quad +\boldsymbol{\beta}_{k+1|k+1}\boldsymbol{K}^{\boldsymbol{b}}_{k+1}\left(\boldsymbol{y}_{k+1}-\hat{\boldsymbol{y}}_{k+1|k}\right) \\ &= \tilde{\boldsymbol{x}}_{k+1|k}+\tilde{\boldsymbol{K}}^{\boldsymbol{x}}_{k+1}(\boldsymbol{y}_{k+1}-\boldsymbol{n}_{k+1})+\boldsymbol{\beta}_{k+1|k+1}\hat{\boldsymbol{b}}_{k+1|k+1} \\ &\quad +\left(\boldsymbol{\beta}_{k+1|k}-\tilde{\boldsymbol{K}}^{\boldsymbol{x}}_{k+1}\boldsymbol{F}^{\mathrm{s}}_{k+1}-\boldsymbol{\beta}_{k+1|k+1}\right)\hat{\boldsymbol{b}}_{k+1|k}\end{aligned} \tag{73}$$

and

$$\hat{\boldsymbol{b}}_{k+1|k+1} = \hat{\boldsymbol{b}}_{k+1|k}+\boldsymbol{K}^{\boldsymbol{b}}_{k+1}\left(\boldsymbol{y}_{k+1}-\hat{\boldsymbol{y}}_{k+1|k}\right) \tag{74}$$

Compute $\boldsymbol{\beta}_{k+1|k+1}$ with (64b) and (68)

$$\begin{aligned}\boldsymbol{\beta}_{k+1|k+1} &= -\boldsymbol{P}^{-1}_1\boldsymbol{P}_2 \\ &= -\tilde{\boldsymbol{P}}^{\boldsymbol{x}}_{k+1|k+1}\left[\boldsymbol{N}^{\mathrm{T}}_{k+1}\boldsymbol{V}^{-1}_k\boldsymbol{F}^{\mathrm{s}}_{k+1}-\left(\tilde{\boldsymbol{P}}^{\boldsymbol{x}}_{k+1|k}\right)^{-1}\boldsymbol{\beta}_{k+1|k}\right] \\ &= \boldsymbol{\beta}_{k+1|k}-\tilde{\boldsymbol{P}}^{\boldsymbol{x}}_{k+1|k+1}\boldsymbol{N}^{\mathrm{T}}_{k+1}\boldsymbol{V}^{-1}_k\boldsymbol{H}_{k+1|k} \\ &= \boldsymbol{\beta}_{k+1|k}-\tilde{\boldsymbol{K}}^{\boldsymbol{x}}_{k+1}\boldsymbol{H}_{k+1|k}\end{aligned} \tag{75}$$

And substitute (75) into (73)

$$\begin{aligned}&\hat{\boldsymbol{x}}_{k+1|k+1} \\ &= \tilde{\boldsymbol{x}}_{k+1|k}+\tilde{\boldsymbol{K}}^{x}_{k+1}(\boldsymbol{y}_{k+1}-\boldsymbol{n}_{k+1})+\boldsymbol{\beta}_{k+1|k+1}\hat{\boldsymbol{b}}_{k+1|k+1} \\ &\quad +\left(-\tilde{\boldsymbol{K}}^{x}_{k+1}\boldsymbol{F}^{\mathrm{s}}_{k+1}+\tilde{\boldsymbol{K}}^{x}_{k+1}\boldsymbol{H}_{k+1|k}\right)\hat{\boldsymbol{b}}_{k+1|k} \\ &= \tilde{\boldsymbol{x}}_{k+1|k+1}+\boldsymbol{\beta}_{k+1|k+1}\hat{\boldsymbol{b}}_{k+1|k+1}\end{aligned} \tag{76}$$

with the definition

$$\tilde{\boldsymbol{x}}_{k+1|k+1} = \tilde{\boldsymbol{x}}_{k+1|k} + \tilde{\boldsymbol{K}}^{x}_{k+1}(\boldsymbol{y}_{k+1} - \tilde{\boldsymbol{y}}_{k+1|k}) \tag{77}$$

where

$$\tilde{\boldsymbol{y}}_{k+1|k} = \sum_{i=0}^{2n} \omega_s^{x(i)} \boldsymbol{h}_{k+1}\left(\boldsymbol{\chi}^{x}_{k+1|k}{}^{(i)}\right) - \boldsymbol{N}_{k+1}\beta_{k+1|k}\hat{\boldsymbol{b}}_{k+1|k} \tag{78}$$

Re-computing $\boldsymbol{P}_{k+1|k+1}$ in (22) yields

$$\boldsymbol{P}^{\boldsymbol{b}}_{k+1|k+1} = \boldsymbol{P}^{\boldsymbol{b}}_{k+1|k} - \boldsymbol{K}^{\boldsymbol{b}}_{k+1}\boldsymbol{P}^{yy}_{k+1|k}\boldsymbol{K}^{\boldsymbol{b}\mathrm{T}}_{k+1} \tag{79}$$

□

Remark 1: The TSUKF is equal to the TSKF when $\boldsymbol{f}(\cdot)$ and $\boldsymbol{h}(\cdot)$ are linear in (1), while it is equal to the UKF when $\boldsymbol{b}_k \equiv \boldsymbol{0}$.

Remark 2: The basic idea of this theorem is the TSKF, so the TSUKF has the same advantages of lower computational cost due to the lower dimensional covariance matrices. By using unscented transformation to handle the non-linear terms, the proposed TSUKF algorithm avoids the calculation of the Jacobian matrix in [19] or in the TSEKF algorithm. Besides, the proposed TSUKF algorithm does not need to compute the sigma points of the bias $\boldsymbol{b}_k$ in the bias filter (3), which is another difference between the proposed TSUKF and the TSUKF in [19].

3 Numerical simulations

3.1 TSUKF-based fault diagnosis strategy

In order to illustrate the theoretical results, without loss of generality, the actuators in closed-loop ACS are three RWs while the sensors are three gyros and two star sensors, and assume that the fault happens in the RW along *x*-axis.

With 3-1-2 rotations, the attitude dynamic and kinematic equations are

$$\begin{cases} \boldsymbol{J}\dot{\boldsymbol{\omega}}_{\mathrm{b}} + \boldsymbol{\omega}_{\mathrm{b}} \times (\boldsymbol{J}\boldsymbol{\omega}_{\mathrm{b}} + \boldsymbol{h}_{\mathrm{act}}) = \boldsymbol{T}_{\mathrm{d}} - \dot{\boldsymbol{h}}_{\mathrm{act}} \\ \dot{\boldsymbol{\phi}}_{\mathrm{bt}} = \boldsymbol{\Phi}\boldsymbol{\omega}_{\mathrm{bt}} \\ \boldsymbol{\omega}_{\mathrm{b}} = \boldsymbol{\omega}_{\mathrm{bt}} + \boldsymbol{A}_{\mathrm{bt}}\boldsymbol{\omega}_{\mathrm{t}} \end{cases}$$

where $\boldsymbol{J} \in R^{3\times 3}$ is the inertia matrix of the spacecraft; $\boldsymbol{T}_{\mathrm{d}} \in R^3$ is the disturbance torque; $\boldsymbol{h}_{\mathrm{act}} \in R^3$ and $\dot{\boldsymbol{h}}_{\mathrm{act}} \in R^3$ are the angular momentum and control torque of the actuators, respectively; $\boldsymbol{\omega}_{\mathrm{b}} \in R^3$ and $\boldsymbol{\omega}_{\mathrm{t}} \in R^3$, respectively, represent the body angular velocity of the spacecraft and the target, relative to the inertial reference frame; $\boldsymbol{\omega}_{\mathrm{bt}} \in R^3$ represents the angular velocity of the satellite body relative to the target reference frame, and the corresponding Euler angles $\boldsymbol{\phi}_{\mathbf{bt}} = [\varphi \quad \theta \quad \psi]^{\mathrm{T}}$; $\boldsymbol{A}_{\mathrm{bt}} \in R^{3\times 3}$ is the corresponding attitude transformation matrix, and $\boldsymbol{A}_{\mathrm{bt}} = \boldsymbol{C}_y(\theta)\boldsymbol{C}_x(\varphi)\boldsymbol{C}_z(\psi)$ where

$$\boldsymbol{C}_y(\theta) = \begin{bmatrix} \cos\theta & 0 & -\sin\theta \\ 0 & 1 & 0 \\ \sin\theta & 0 & \cos\theta \end{bmatrix}$$

$$\boldsymbol{C}_x(\varphi) = \begin{bmatrix} 1 & 0 & 0 \\ 0 & \cos\varphi & \sin\varphi \\ 0 & -\sin\varphi & \cos\varphi \end{bmatrix}$$

$$\boldsymbol{C}_z(\psi) = \begin{bmatrix} \cos\psi & \sin\psi & 0 \\ -\sin\psi & \cos\psi & 0 \\ 0 & 0 & 1 \end{bmatrix}$$

and

$$\boldsymbol{\Phi} = \frac{1}{\cos\varphi}\begin{bmatrix} \cos\theta\cos\varphi & 0 & \sin\theta\cos\varphi \\ \sin\varphi\sin\theta & \cos\varphi & -\sin\varphi\cos\theta \\ -\sin\theta & 0 & \cos\theta \end{bmatrix}$$

Defining $\boldsymbol{x} = \begin{bmatrix}\boldsymbol{\omega}_{\mathrm{b}}^{\mathrm{T}} & \boldsymbol{\phi}_{\mathrm{bt}}^{\mathrm{T}}\end{bmatrix}^{\mathrm{T}} \in R^6$ as the system state vector, the state equation of satellite attitude control system can be given as

$$\dot{\boldsymbol{x}} = \boldsymbol{g}(\boldsymbol{x}) + \boldsymbol{B}u + \boldsymbol{F}^{\mathrm{a}}\boldsymbol{b} + \boldsymbol{w}^{\boldsymbol{x}} \tag{80}$$

where

$$\boldsymbol{g}(\boldsymbol{x}) = \begin{bmatrix} \boldsymbol{0} \\ \dot{\boldsymbol{\phi}}_{\mathrm{bt}}(\boldsymbol{x}) \end{bmatrix}$$

$$\dot{\boldsymbol{\phi}}_{\mathrm{bt}}(\boldsymbol{x}) = \boldsymbol{\Phi}(\boldsymbol{x})\boldsymbol{\omega}_{\mathrm{b}} - \boldsymbol{\Phi}(\boldsymbol{x})\boldsymbol{A}_{\mathrm{bt}}(\boldsymbol{x})\boldsymbol{\omega}_{\mathrm{t}}$$

$$\boldsymbol{B} = \begin{bmatrix} \boldsymbol{J}^{-1} \\ \boldsymbol{0} \end{bmatrix}$$

where $\boldsymbol{B} \in R^{6\times 3}$ is the control input matrix; $\boldsymbol{u} \in R^3$ is the control input vector, and $\boldsymbol{u} = -\boldsymbol{\omega}_{\mathrm{b}} \times (\boldsymbol{J}\boldsymbol{\omega}_{\mathrm{b}} + \boldsymbol{h}_{\mathrm{act}}) - \dot{\boldsymbol{h}}_{\mathrm{act}}$; $\boldsymbol{b} \in R^3$ is the fault vector, and $\dot{\boldsymbol{b}} = \boldsymbol{w}^{\boldsymbol{b}}$ where $\boldsymbol{w}^{\boldsymbol{b}}$ is the white Gaussian process noise with zero mean; $\boldsymbol{F}^{\mathrm{a}} \in R^{6\times 3}$ is the actuator fault distribution matrix; $\boldsymbol{w}^{\boldsymbol{x}}$ is the white Gaussian process noise with zero mean.

The observation equation is given by

$$\boldsymbol{y} = \boldsymbol{C}x + \boldsymbol{F}^{\mathrm{s}}\boldsymbol{b} + \boldsymbol{v} \tag{81}$$

where $\boldsymbol{y} \in R^6$ is the measurement vector; $\boldsymbol{C} \in R^{6\times 6}$ is the output matrix, and $\boldsymbol{C} = \boldsymbol{I}_6$ where $\boldsymbol{I}_n \in R^{n\times n}$ is the unit matrix with n dimensions; $\boldsymbol{F}^{\mathrm{s}} \in R^{6\times 3}$ is the sensor fault distribution matrix; $\boldsymbol{v}$ is the white Gaussian measurement noise with zero mean. Discretising (80) and (81), the system model with faults can be written as

$$\begin{cases} \boldsymbol{x}_{k+1} = \boldsymbol{g}_k(\boldsymbol{x}_k) + \boldsymbol{B}_k\boldsymbol{u}_k + \boldsymbol{F}^{\mathrm{a}}_k\boldsymbol{b}_k + \boldsymbol{w}^{\boldsymbol{x}}_k \\ \boldsymbol{b}_{k+1} = \boldsymbol{b}_k + \boldsymbol{w}^{\boldsymbol{b}}_k \\ \boldsymbol{y}_k = \boldsymbol{C}_k\boldsymbol{x}_k + \boldsymbol{F}^{\mathrm{s}}_k\boldsymbol{b}_k + \boldsymbol{v}_k \end{cases} \tag{82}$$

where $\boldsymbol{b}_k \in R^3$ is the fault vector.

When considering actuator faults only, $\boldsymbol{F}^{\mathrm{s}}_k = \boldsymbol{0}_{6\times 3}$. For additive faults, $\boldsymbol{b}_k$ represents the magnitude of additive faults of actuators and leads to an output torque with a bias, i.e. $\boldsymbol{T}^{\mathrm{out}} = \boldsymbol{T}^{\mathrm{cmd}} + \boldsymbol{b}_k$ where $\boldsymbol{T}^{\mathrm{out}}$ is the output torque of the actuators, and $\boldsymbol{T}^{\mathrm{cmd}}$ is the command torque of the actuators. Thus, the additive fault distribution matrix $\boldsymbol{F}^{\mathrm{a,add}}_k$ can be given by

$$\boldsymbol{F}^{\mathrm{a,add}}_k = -\boldsymbol{B}_k \tag{83}$$

For multiplicative faults, $\boldsymbol{b}_k$ represents the degree of multiplicative faults of actuators and causes an output torque with a loss factor, i.e. $\boldsymbol{T}_{\mathrm{out}} = [\boldsymbol{I}_3 - \mathrm{diag}(\boldsymbol{b}_k)]\boldsymbol{T}_{\mathrm{cmd}}$. So the multiplicative fault distribution matrix $\boldsymbol{F}^{\mathrm{a,mul}}_k$ can be given by

$$\boldsymbol{F}^{\mathrm{a,mul}}_k = \boldsymbol{B}_k\mathrm{diag}\left(\dot{\boldsymbol{h}}_{\mathrm{act}_{\mathrm{cmd}}k}\right) \tag{84}$$

where $\dot{\boldsymbol{h}}_{\mathrm{act}_{\mathrm{cmd}}k} \in R^3$ is the command torque of actuators in the kth step. In general, the unknown bias $\boldsymbol{b}_k$ describes the loss of control effectiveness. If the actuator faults are treated as additive faults, $\boldsymbol{F}^{\mathrm{a}}_k = \boldsymbol{F}^{\mathrm{a,add}}_k$; if they are treated as multiplicative faults, $\boldsymbol{F}^{\mathrm{a}}_k = \boldsymbol{F}^{\mathrm{a,mul}}_k$. Similarly, when considering sensor faults only, $\boldsymbol{F}^{\mathrm{a}}_k = \boldsymbol{0}_{6\times 3}$, and the sensor fault distribution matrix $\boldsymbol{F}^{\mathrm{s}}_k$ can be obtained in the same way.

For the system described in (82), the attitude information and the actuator faults can be estimated using the TSUKF, where the actuator fault is treated as bias.

For stabilisation attitude control, the theoretical control torque given by the RW is essentially 0 and therefore the multiplicative faults cannot impact on the ACS. That is, only additive faults need to be taken into account and the fault distribution matrix is given by (83) when applying TSUKF. Furthermore, for attitude stabilisation control, the ACS can be approximated as a linear system due to the small nature of Euler angles. In this case, the performance of TSUKF is not better than that of TSKF or TSEKF.

When tracking a manoeuvring target, the theoretical control torque $\boldsymbol{u}_k$ given by the RW is dynamic, which means that both of the additive faults and multiplicative faults have influence on the ACS. However, it is hard to judge whether the fault is an additive fault or a multiplicative fault in actual control system, and thereby the fault distribution matrix $\boldsymbol{F}_k^{\mathrm{a}}$ is uncertain. Fortunately, the influence of the multiplicative faults on the system could be measured by the estimation of the faults magnitude via the TSUKF-based estimator; similarly, the influence of additive faults could be estimated as the loss factors of control effectiveness, too. Thereby, TSUKF-based estimator with two kinds of fault distribution matrices can be used to estimate the faults, even though the type of the faults is unknown.

3.2 Simulation parameters

Two simulation backgrounds are taken into account: attitude stabilisation control and attitude tracking control. The ACS can be treated as linear systems approximately in the former case in which the control torque is near zero. To estimate the multiplicative fault for the RWs, the spacecraft ACS must satisfy the persistent excitation condition. In other words, the spacecraft must be manoeuvring or tracking a target to ensure the RWs are activated.

Considering the limitation of paper length, two kinds of actuator faults and only additive faults of the gyros are considered in the following simulations. The additive and multiplicative faults parameters are given as follows.

Case 1: The first RW fault's magnitude $\boldsymbol{b}_1 = [0.010 \quad 0 \quad 0]^{\mathrm{T}}\,\mathrm{N\cdot m}$ exists during the period $100\,\mathrm{s} \le t_1 < 150\,\mathrm{s}$, and the second one $\boldsymbol{b}_2 = [0.015 \quad 0 \quad 0]^{\mathrm{T}}\,\mathrm{N\cdot m}$ exists during the period $150\,\mathrm{s} \le t_2 < 200\,\mathrm{s}$.

Case 2: The control effectiveness factors of the first RW fault $\boldsymbol{b}_1 = [0.2 \quad 0 \quad 0]^{\mathrm{T}}$ exist during the period $100\,\mathrm{s} \le t_1 < 150\,\mathrm{s}$, and those of the second RW fault $\boldsymbol{b}_2 = [0.4 \quad 0 \quad 0]^{\mathrm{T}}$ exists during the period $150\,\mathrm{s} \le t_2 < 200\,\mathrm{s}$.

Case 3: The gyro fault's magnitude $\boldsymbol{b} = [0.2 \quad 0 \quad 0]^{\mathrm{T}}{}^{\circ}/\mathrm{s}$ exists during the period $100\,\mathrm{s} \le t < 200\,\mathrm{s}$.

The system parameters and initial values in the simulation are chosen as follows. The maximum output torque of the RWs is $0.2\,\mathrm{N\cdot m}$ and the maximum angular momentum is $2\,\mathrm{N\cdot m\cdot s}$. The spacecraft inertia matrix is $\boldsymbol{J} = \mathrm{diag}([17 \quad 12 \quad 10])\,\mathrm{kg\cdot m^2}$. Defining $\boldsymbol{\phi}_1 = \boldsymbol{\Phi}$ and $\boldsymbol{\phi}_2 = \boldsymbol{\Phi}\boldsymbol{A}_{\mathrm{bt}}$, the controller is

$$\boldsymbol{u}_k = \boldsymbol{J}\boldsymbol{\phi}_{1k}^{-1} \times \left[-\boldsymbol{C}_1\dot{\boldsymbol{\phi}}_k - \boldsymbol{C}_2\boldsymbol{\phi}_k + \dot{\boldsymbol{\phi}}_{2k}\boldsymbol{\omega}_{\mathrm{t}k} + \boldsymbol{\phi}_{2k}\dot{\boldsymbol{\omega}}_{\mathrm{t}k} - \dot{\boldsymbol{\phi}}_{1k}\boldsymbol{\omega}_{\mathrm{b}k}\right]$$

where

$$\boldsymbol{C}_1 = 0.54\boldsymbol{I}_3$$
$$\boldsymbol{C}_2 = 0.09\boldsymbol{I}_3$$
$$\boldsymbol{\phi}_1^{-1} = \begin{bmatrix} \cos\theta & 0 & -\cos\varphi\sin\theta \\ 0 & 1 & \sin\varphi \\ \sin\theta & 0 & \cos\varphi\cos\theta \end{bmatrix}$$

Relative to the inertial reference frame, the Euler angles of the stable target are $\boldsymbol{\phi}_{\mathrm{t}} = [0 \quad 0 \quad 0]^{\mathrm{T}}\,\mathrm{rad}$, and the Euler angles of the manoeuvring target are

$$\boldsymbol{\phi}_{\mathrm{t}} = \left[\frac{\pi}{6}\sin\left(\frac{2\pi}{100}t\right) \quad \frac{\pi}{60}\sin\left(\frac{2\pi}{100}t\right) \quad \frac{\pi}{60}\cos\left(\frac{2\pi}{100}t\right)\right]^{\mathrm{T}}\,\mathrm{rad}$$

The initial Euler angles of the spacecraft relative to the attitude coordinate system of the manoeuvring target are $\boldsymbol{\phi}_{\mathrm{bt0}} = \left[\frac{\pi}{6} \quad 0 \quad 0\right]^{\mathrm{T}}\,\mathrm{rad}$, and the initial angular velocity vector relative to the inertial coordinate system is $\boldsymbol{\omega}_{\mathbf{b0}} = [0 \quad 0 \quad 0]^{\mathrm{T}}\,\mathrm{rad/s}$. The initial transfer matrix is $\boldsymbol{P}_0^{\boldsymbol{x}} = \boldsymbol{I}_6$. The process noise covariance matrices are

$$\boldsymbol{W}^{\boldsymbol{x}} = \begin{bmatrix} \sigma_{\boldsymbol{\omega}}^2\boldsymbol{I}_3 & \\ & \sigma_{\boldsymbol{\phi}}^2\boldsymbol{I}_3 \end{bmatrix}, \quad \boldsymbol{W}^{\boldsymbol{b}} = \sigma_{\mathrm{a}}^2\boldsymbol{I}_3$$

where $\sigma_{\boldsymbol{\omega}} = 1\times10^{-5}\,\mathrm{rad/s}$, $\sigma_{\boldsymbol{\phi}} = 1\times10^{-5}\,\mathrm{rad}$. For the fault distribution matrix (83), $\sigma_{\mathrm{a}} = 1\times10^{-4}\,\mathrm{N\cdot m}$; for the fault distribution matrix (84), $\sigma_{\mathrm{a}} = 1\times10^{-3}$. The measurement noise covariance matrix is $\boldsymbol{V} = (1\times10^{-5})^2\boldsymbol{I}_6$. The disturbance torque is

$$\boldsymbol{T}_{\mathrm{d}} = A_0\begin{bmatrix} 3\cos\omega_{\mathrm{orbit}}t + 1 \\ 1.5\sin\omega_{\mathrm{orbit}}t + 3\cos\omega_{\mathrm{orbit}}t \\ 3\sin\omega_{\mathrm{orbit}}t + 1 \end{bmatrix}$$

where $A_0 = 1.5\times10^{-5}\,\mathrm{N\cdot m}$, and $\omega_{\mathrm{orbit}} = 0.001\,\mathrm{rad/s}$. During the estimation, $\alpha = 1\times10^{-3}$. The the simulating step time is 0.01 s.

3.3 Simulation results

3.3.1 Attitude stabilisation control in case 1: For attitude stabilisation control, the faults are set under case 1 only. For actuator faults only, $\boldsymbol{F}_k^{\mathrm{s}} = \boldsymbol{0}$; when the faults are treated as additive faults, $\boldsymbol{F}_k^{\mathrm{a}} = \boldsymbol{F}_k^{\mathrm{a,add}}$ where $\boldsymbol{F}_k^{\mathrm{a,add}}$ is shown in (83), while when they are treated as multiplicative faults, $\boldsymbol{F}_k^{\mathrm{a}} = \boldsymbol{F}_k^{\mathrm{a,mul}}$ where $\boldsymbol{F}_k^{\mathrm{a,mul}}$ is shown in (84). The simulation results are given in Fig. 1.

The estimations of the Euler angles are shown in Fig. 1*a* while the estimations of the angular velocity are shown in Fig. 1*b*. During the period that the two faults happened, the Euler angles in *x*-axis are -0.372° and -0.560°, respectively. During the period without fault, the Euler angle in *x*-axis is 0°. Obviously, the faults result in the control torque's changes in the RW along the *x*-axis so that there exist Euler angle biases in the *x*-axis.

Fig. 1*c* presents the bias estimation results using (83). In particular, in Fig. 1*c*, the additive fault along the *x*-axis changes at 100, 150 and 200 s, and the estimation values converge to 0.010, 0.015 and $0\,\mathrm{N\cdot m}$ with the mean square errors (MSEs) 1.01×10^{-8}, 9.53×10^{-9} and 7.18×10^{-9}, respectively.

3.3.2 Attitude tracking control in case 1: For attitude tracking control, the proposed TSUKF algorithm is applied to estimate the state and the bias, and the fault distribution matrices are same as those in the previous simulation. The faults in this set of simulation are set in case 1 (shown in Fig. 2).

For attitude tracking control, the bias estimation for case 1, representing the fault magnitude, are shown in Fig. 2*a*. Particularly, the estimation value along the *x*-axis converge to 0.010, 0.015 and $0\,\mathrm{N\cdot m}$ with the MSEs 1.49×10^{-8}, 1.29×10^{-8}, and 1.25×10^{-8}, respectively. Certainly, the loss of control effectiveness factors shown in Fig. 2*b*, which can measure the degree of the actuator failures, can be obtained by function fitting.

The Euler angles are shown in Fig. 2*c* while the angular velocity is shown in Fig. 2*d*. As same as the results in Fig. 1*a*, the relative attitude of the *x*-axis was changed by the two faults with the biases of -0.372° and -0.560°, respectively. After the faults disappeared, the relative attitude of the *x*-axis converged to 0°, again.

3.3.3 Attitude tracking control in case 2: For attitude tracking control, the faults in this set of simulation are set in case 2, and the

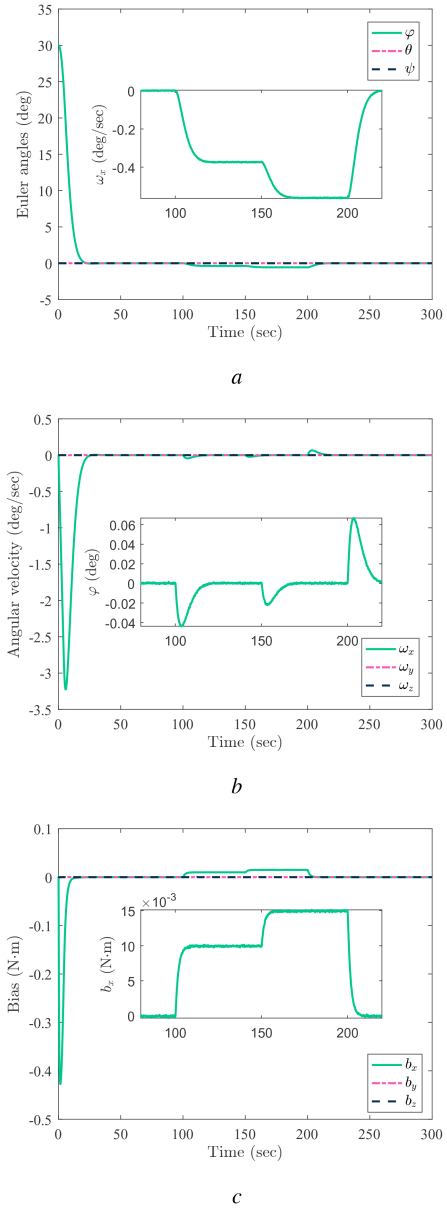

Fig. 1 *Simulation results of attitude stabilisation control in case 1*
(a) Euler angles, ***(b)*** Angular velocity, ***(c)*** RW bias estimation using (83)

fault distribution matrices are same as those in the previous simulation, too. Figs. 3*a* and *b* present the bias estimations using the TSUKF with fault distribution matrix (83) and (84), respectively. While the Euler angles and the angular velocity are shown in Figs. 3*c* and *d*, respectively.

Shown in Fig. 3*b*, the fault of the *x*-axis changes at 100, 150 and 200 s, and the estimation value converges to 0.2, 0.4 and 0 with the MSEs 1.40×10^{-6}, 8.19×10^{-6} and 8.50×10^{-6}, respectively. Similarly, the bias estimation result shown in Fig. 3*a* can be used to measure the magnitude of the fault by function fitting. The difference between the results and the real values along the other two axes is due to two reasons. First, the disturbances and noises in the system were regarded as biases and they are estimated by the TSUKF. Second, the actuator fault happened on the *x*-axis affected the performance of the other two axes, and the influence would disappear if the fault continued to be exist as time went by.

From the estimation results, it is obvious that $-\boldsymbol{U}_k\boldsymbol{b}_k^{\text{mul}}=\boldsymbol{b}_k^{\text{add}}$ for the same fault, which is consistent with the fault modelling (83) and (84). No matter the faults are additive or multiplicative, TSUKF can be used to estimate the bias using the fault distribution matrix in both (83) and (84) because the two kinds of estimation results are different ways to characterise the same fault information. In addition, the precision of TSUKF is higher than that of TSEKF presented in our previous work [20].

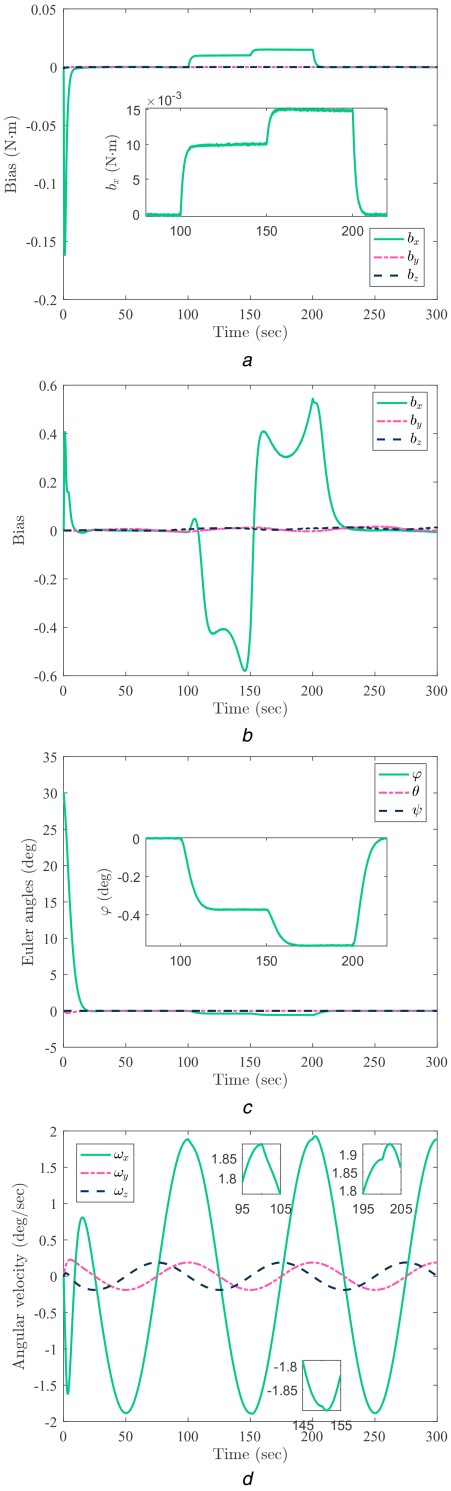

Fig. 2 *Simulation results of attitude tracking control in case 1*
(a) RW bias estimation using (83), ***(b)*** RW bias estimation using (84), ***(c)*** Euler angles, ***(d)*** Angular velocity

3.3.4 Attitude tracking control in both case 1 and case 3: For attitude tracking control, the faults are set in both case 1 and case 3 where RW faults and gyro faults exist at the same time. Limited by the paper length, the simulation results where the faults are treated as additive faults are shown in Fig. 4 only. When both actuator and sensor faults exist, the bias vector $\boldsymbol{b}_k$ is $\boldsymbol{b}_k=[(\boldsymbol{b}_k^{\text{a}})^{\text{T}},(\boldsymbol{b}_k^{\text{s}})^{\text{T}}]^{\text{T}}$, and the additive fault distribution matrices $\boldsymbol{F}_k^{\text{a, add}}$ and $\boldsymbol{F}_{k+1}^{\text{s, add}}$ are written as

$$\boldsymbol{F}_k^{\text{a, add}}=[\boldsymbol{B}_k\quad\boldsymbol{0}],\quad \boldsymbol{F}_{k+1}^{\text{s, add}}=\begin{bmatrix}\boldsymbol{0}&\boldsymbol{I}_3\\ \boldsymbol{0}&\boldsymbol{0}\end{bmatrix}$$

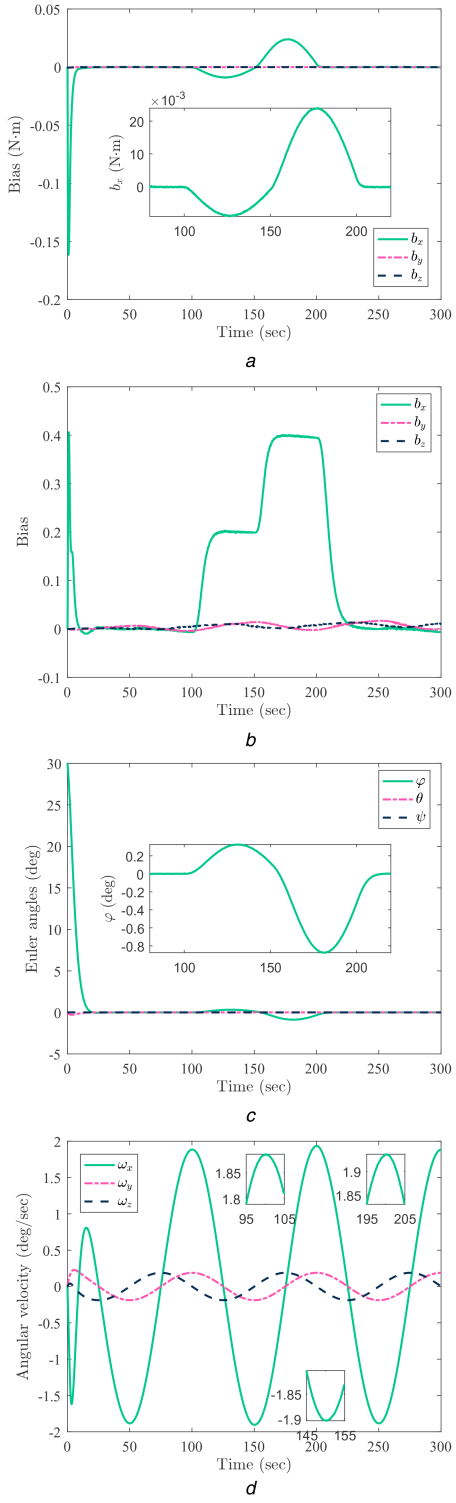

Fig. 3 *Simulation results of attitude tracking control in case 2*
(a) RW bias estimation using (83), ***(b)*** RW bias estimation using (84), ***(c)*** Euler angles, ***(d)*** Angular velocity

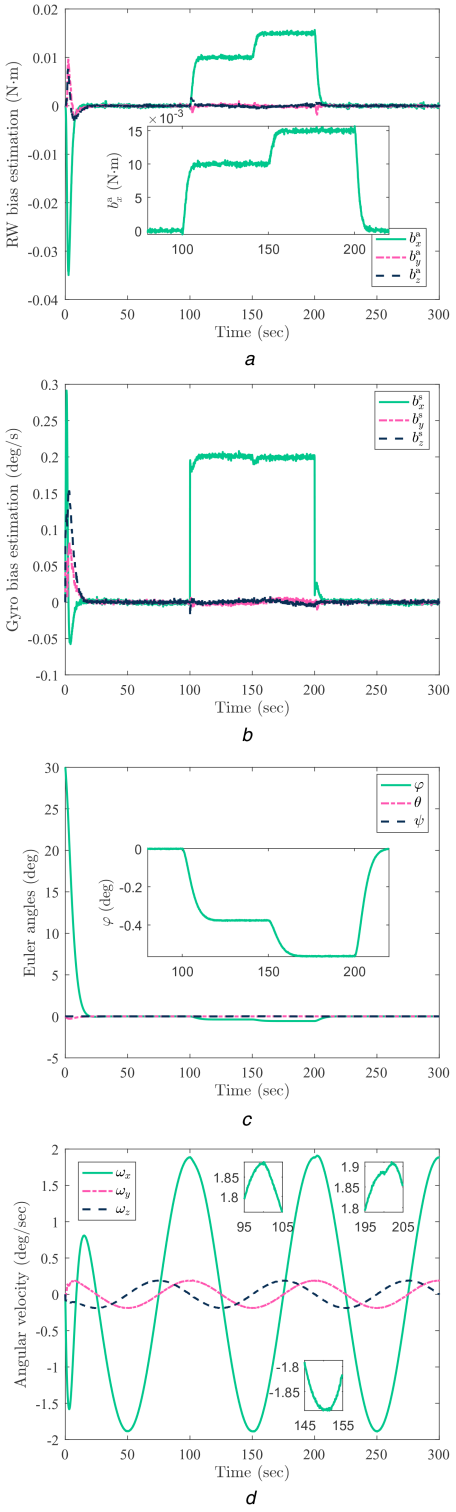

Fig. 4 *Simulation results of attitude tracking control in both case 1 and case 3*
(a) Detailed RW bias estimation, ***(b)*** Detailed gyro bias estimation, ***(c)*** Euler angles, ***(d)*** Angular velocity

$\boldsymbol{W}^b = \mathrm{diag}(\sigma_\mathrm{a}^2\boldsymbol{I}_3,\ \sigma_\mathrm{s}^2\boldsymbol{I}_3)$ where $\sigma_\mathrm{a} = 1\times10^{-4}\,\mathrm{N\cdot m}$, and $\sigma_\mathrm{s} = 1\times10^{-4}\,\mathrm{rad/s}$.

For the sake of clarity, the bias estimation result $\boldsymbol{b}_k = [b_1\ \ b_2\ \ b_3\ \ b_4\ \ b_5\ \ b_6]_k^\mathrm{T}$ is divided into two parts: the former part – the magnitude of the RW faults, $\boldsymbol{b}_k^\mathrm{a} = [b_1\ \ b_2\ \ b_3]_k^\mathrm{T} = \left[b_x^\mathrm{a}\ \ b_y^\mathrm{a}\ \ b_z^\mathrm{a}\right]_k^\mathrm{T}$, is shown in Fig. 4*a* while the latter part – the magnitude of the gyro faults, $\boldsymbol{b}_k^\mathrm{s} = [b_4\ \ b_5\ \ b_6]_k^\mathrm{T} = \left[b_x^\mathrm{s}\ \ b_y^\mathrm{s}\ \ b_z^\mathrm{s}\right]_k^\mathrm{T}$, is presented in Fig. 4*b*. The attitude informations are shown in Figs. 4*c* and *d*.

As shown in Fig. 4*a*, for actuator faults, the estimation value along the *x*-axis converge to 0.010, 0.015 and $0\,\mathrm{N\cdot m}$, respectively. As shown in Fig. 4*b*, for sensor faults, the estimation value along the *x*-axis converge to 0.2 and 0°/s, respectively. It is obvious that the actuator and sensor faults influence the results of each other.

4 Conclusions

This paper investigates the RW fault estimation based on the TSUKF.

Based on the separate-bias principle, a novel TSUKF algorithm was proposed, which not only can estimate the attitude angular velocity and the Euler angles, but also can estimate the RW faults no matter they are bias ones or losses of the control effectiveness factor.

The TSUKF in this paper can be applied to the estimation of both additive faults and multiplicative faults for the RW in satellite attitude control system. Unlike EKF or TSEKF, the model of non-linear system was directly used by the TSUKF in the filtering process, without the necessity to be extended. The simulation results verified that the TSUKF algorithm was feasible for both attitude stabilisation and tracking control.

However, the TSUKF algorithm is only applicable to the case with bias linearisation. In the non-linear system model with non-linear bias, the augmented UKF is more convenient. While in the non-linear system model with linear bias, lower dimensional vectors and matrices need to be computed in the TSUKF algorithm, leading to lower computational cost.

5 Acknowledgments

This work was supported by the National Key Research and Development Plan, People's Republic of China [grant number 2016YFB0500901].

6 References

[1] Friedland, B.: 'Treatment of bias in recursive filtering', *IEEE Trans. Autom. Control*, 1969, **14**, pp. 359–367

[2] Alouani, A.T., Xia, P., Rice, T.R., *et al.*: 'On the optimality of two-stage state estimation in the presence of random bias', *IEEE Trans. Autom. Control*, 1993, **38**, pp. 1279–1283

[3] Keller, J.Y., Darouach, M.: 'Optimal two-stage Kalman filter in the presence of random bias', *Automatica*, 1997, **33**, pp. 1745–1748

[4] Keller, J.Y., Sauter, D.: 'Kalman filter for discrete-time stochastic linear systems subject to intermittent unknown inputs', *IEEE Trans. Autom. Control*, 2013, **58**, pp. 1882–1887

[5] Hsieh, C.S.: 'Robust two-stage Kalman filters for systems with unknown inputs', *IEEE Trans. Autom. Control*, 2000, **45**, pp. 2374–2378

[6] Khabbazi, M.R., Esfanjani, R.M.: 'Robust two-stage Kalman filtering with state constraints'. 2015 23rd Iranian Conf. on Electrical Engineering (ICEE), Tehran, Iran, May 2015, pp. 1036–1041

[7] Hajiyev, C.: 'Two-stage Kalman filter-based actuator/surface fault identification and reconfigurable control applied to F-16 fighter dynamics', *Int. J. Adapt. Control Signal Process.*, 2013, **27**, pp. 755–770

[8] Wang, J., Qi, X.: 'Fault diagnosis for flight control systems using subspace method and adaptive two-stage Kalman filter', *Trans. Inst. Meas. Control*, 2016, **38**, pp. 1480–1490

[9] Qian, H., Huang, W., Qian, L., *et al.*: 'Robust extended Kalman filter for attitude estimation with multiplicative noises and unknown external disturbances', *IET Control Theory Applic.*, 2014, **8**, pp. 1523–1536

[10] Inoue, R.S., Terra, M.H., Cerri, J.P.: 'Extended robust Kalman filter for attitude estimation', *IET Control Theory Applic.*, 2016, **10**, pp. 162–172

[11] Xiao, Q., Wu, Y., Fu, H., *et al.*: 'Two-stage robust extended Kalman filter in autonomous navigation for the powered descent phase of Mars EDL', *IET Signal Process.*, 2015, **9**, pp. 277–287

[12] Xiao, M., Zhang, Y., Wang, Z., *et al.*: 'Augmented robust three-stage extended Kalman filter for Mars entry-phase autonomous navigation', *Int. J. Syst. Sci.*, 2018, **49**, pp. 27–42

[13] Julier, S.J., Uhlmann, J.K., Durrant-Whyte, H.F.: 'A new approach for filtering nonlinear systems'. Proc. of the 1995 American Control Conf., Seattle, WA, USA, June 1995, vol. 3, pp. 1628–1632

[14] Rahimi, A., Kumar, K.D., Alighanbari, H.: 'Fault estimation of satellite reaction wheels using covariance based adaptive unscented Kalman filter', *Astronautica*, 2017, **134**, pp. 159–169

[15] Chatterjee, S., Sadhu, S., Ghoshal, T.K.: 'Fault detection and identification of non-linear hybrid system using self-switched sigma point filter bank', *IET Control Theory Applic.*, 2015, **9**, pp. 1093–1102

[16] Xiao, M., Zhang, Y., Fu, H.: 'Three-stage unscented Kalman filter for state and fault estimation of nonlinear system with unknown input', *J. Franklin Inst.*, 2017, **354**, pp. 8421–8443

[17] Farina, A., Ristic, B., Benvenuti, D.: 'Tracking a ballistic target: comparison of several nonlinear filters', *IEEE Trans. Aerosp. Electron. Syst.*, 2002, **38**, pp. 854–867

[18] Chang, L., Hu, B., Chang, G., *et al.*: 'Marginalised iterated unscented Kalman filter [Brief Paper]', *IET Control Theory Applic.*, 2012, **6**, pp. 847–854

[19] Xu, J., Jing, Y., Dimirovski, G.M., *et al.*: 'Two-stage unscented Kalman filter for nonlinear systems in the presence of unknown random bias'. American Control Conf., Seattle, WA, USA, June 2008, pp. 3530–3535

[20] Chen, X., Sun, R., Jiang, W., *et al.*: 'A novel two-stage extended Kalman filter algorithm for reaction flywheels fault estimation', *Chin. J. Aeronaut.*, 2016, **29**, pp. 462–469